Dynamic Mode Decomposition Application to Dominance Ratio Assessment in Monte Carlo *k*-Eigenvalue Calculation

Toshihiro Yamamoto[a*], Xiuzhong Shen[a], Hiroki Sakamoto[b]

[a]*Institute for Integrated Radiation and Nuclear Science, Kyoto University, 2 Asashiro Nishi, Kumatori-cho, Sennan-gun, Osaka, 590–0494, Japan*
[b]*Independent researcher, Radiation Dose Analysis and Evaluation Network, 4–13–14, Kokubunji-shi, Tokyo, 185–0001, Japan*

Abstract

Dynamic mode decomposition (DMD) is applied to assess the dominance ratio (the ratio of the second-largest to the largest *k*-eigenvalue) from the fission source convergence during Monte Carlo power iterations. The fission source transition in each discretized tally region toward convergence is viewed as snapshots for DMD analysis. DMD is found to yield satisfactory results for the dominance ratio when various arbitrary parameters are selected, even for systems that have a dominance ratio that is very close to unity (~0.999). The accuracy of the method depends on the parameters, especially in a system that has a low dominance ratio due to a reduced number of cycles before convergence. The spatial discretization of tally regions where fission sources accumulate can be coarse, in contrast to that in the fission matrix method, which is an advantage of the proposed method.

Keywords: Dynamic mode decomposition; Monte Carlo; Eigenvalue calculation; Dominance ratio

1. Introduction

The power iteration method is a commonly used technique for calculating the neutron effective multiplication factor, k_{eff}, in both deterministic and stochastic (Monte Carlo) calculation methods. A guessed initial fission source distribution eventually reaches the fundamental mode distribution through successive fission generations (cycles). The number of power iterations that are necessary for fission source convergence is dominated by the dominance

[*] Corresponding author
E-mail address: yamamoto.toshihiro.8u@kyoto-u.ac.jp (T. Yamamoto)

ratio. The dominance ratio is defined as the ratio of the second-largest to the largest *k*-eigenvalue. The dominance ratio is an important index for the stability of the neutron flux distribution in a power reactor. Neither the second-largest *k*-eigenvalue nor the dominance ratio can be straightforwardly calculated with the Monte Carlo method.

Many studies have been conducted to calculate the second eigenvalue or the dominance ratio with the Monte Carlo method. As a method for calculating the second and higher mode eigenvalues, the modified power method (MPM) was proposed by Booth (2003, 2006). The method calculates higher eigenmodes by keeping the positive and negative components growing at the same rate. The MPM was further studied by Yamamoto (2009) and was extended by introducing the "transfer matrix" method (Zhang, et al., 2016, 2018). One of the difficulties in the MPM is that the method requires that the positive and negative particle weights cancel out in finely discretized regions. The cancellation cannot be performed without an intentionally designed Monte Carlo technique. The currently available technique for cancellation is an approximate way requiring that the entire fission region be finely discretized.

The fission matrix method (FMM) is a method for calculating higher eigenmodes without introducing negative particle weights (Dufek and Gudowski, 2009; Carney et al., 2014; Terlizzi and Kotlyar, 2019). The fission matrix can be estimated before the fission source distribution has fully converged, which is one of the advantages over other techniques for dominance ratio assessment. However, the spatial discretization for the FMM needs to be fine enough to obtain a sufficiently accurate dominance ratio. The requirement for the fine resolution of the fission matrix increases the computational burden, thereby limiting the applicability of FMM to a subset of problems.

In a different dominance ratio assessment approach, the time series analysis technique is applied to the correlation of fission sources between successive fission cycles because the degree of the correlation is closely related to the dominance ratio (Ueki et al., 2003; Ueki et al., 2004; Nease and Ueki, 2007; Nease and Ueki, 2009). This method, which is named the coarse mesh projection method (CMPM), uses autoregressive-moving average fitting. In contrast to the FMM, the CMPM enables the eigenvalue ratios to be extracted even with very coarse mesh schemes. The disadvantage of the CMPM is that the time series data cannot be accumulated until the fission source has fully converged. A method for circumventing this difficulty in the CMPM was developed, which is called the noise propagation matrix method (NPMM) (Sutton et al., 2011). While the NPMM has the same coarse-mesh accuracy as the CMPM, the NPMM can estimate the dominance ratio using the time series data before fission source convergence.

A simple method that was proposed by Gorodkov (2011) calculates the dominance ratio by imposing a black boundary condition on a symmetry plane where the flux of the 1st eigenmode is zero. If a core geometry is symmetric, the zero-flux plane can be easily found. A strategy for estimating the dominance ratio for some nonsymmetrical systems was also proposed.

In a previous work on dominance ratio assessment (Dumonteil and Courau, 2010), which is highly similar to this study, the convergence process of the fission source is fitted to $a \cdot \exp(-bn) + c$, where a and c are the fitting constants, n is the cycle number, and b is the natural logarithm of the dominance ratio. The disadvantage of this method is contamination by eigenmodes that are higher than the 1st mode. Similar problems are encountered in the fitting process of subcriticality measurement in the pulsed neutron method or Rossi-α method. Recently, dynamic mode decomposition (DMD) (Schmid, 2010; Kutz et al., 2016) was introduced to extract the fundamental mode and major higher eigenmodes from measured data in the pulsed neutron method (McClarren, 2019; Hardy et al., 2019) and the Rossi-α method (Yamamoto and Sakamoto, 2022).

DMD is a technique for decomposing a complex system. DMD was originally developed for fluid dynamics analyses and is now gradually becoming a popular technique in the nuclear engineering field. Examples of DMD applications in the nuclear engineering field include the evolution of spatially varying nuclide compositions in a reactor (Abdo et al., 2019), acceleration of discrete ordinates radiative transfer calculations (McClarren and Haut, 2020), reactor stability analysis of a coupling system between neutronics and thermal hydraulics (Di Ronco et al., 2020), and eigenmode analyses in subcriticality measurements (McClarren, 2019; Hardy et al., 2019;

Yamamoto and Sakamoto, 2021).

Roberts et al. (2019) applied DMD to accelerate the power iteration method for k-eigenvalue calculations by viewing successive power iterations as snapshots of a time-varying system. Roberts et al. addressed the acceleration of deterministic k-eigenvalue calculations that used the finite-volume approximation. The objective of the present study is to extend the approach of Dumonteil and Courau (2010) and Roberts et al. (2019) by applying DMD to dominance ratio assessment in Monte Carlo k-eigenvalue calculations, thereby suppressing the influence of eigenmodes that are higher than the 1st mode.

The remainder of this paper is organized as follows. In Section 2, the fundamentals of the power iteration method and the preparation of snapshots of the fission source distribution for DMD analysis are presented. In Section 3, a brief overview of DMD and its application in this study is presented. In Section 4, numerical examples in which dominance ratios are calculated using DMD are presented. The final section presents the conclusions and recommendations for future work.

2. Dominance ratio in the Monte Carlo power iteration method

The theory and procedure for dominance ratio assessment in the Monte Carlo power iteration method are presented in this section. In this study, the power iteration method follows a standard procedure that is adopted in widely available Monte Carlo calculation codes. The procedure is fundamentally the same as that in the deterministic approach that was published in (Roberts et al., 2019).

At the beginning of a Monte Carlo k-eigenvalue calculation, an initial fission source distribution $F_0(\boldsymbol{r})$ is assigned to the calculation domain. The volume integral of $F_0(\boldsymbol{r})$ over the entire domain is expressed as follows:

$$N = \int_V F_0(\boldsymbol{r}) d\boldsymbol{r}, \tag{1}$$

where N is the nominal number of fission neutrons (total source weight) in each cycle, which is constant throughout the calculation. The initial fission source distribution $F_0(\boldsymbol{r})$ can be expressed as a linear combination of the eigenfunctions as follows:

$$F_0(\boldsymbol{r}) = \sum_{i=0}^{\infty} a_i \varphi_i(\boldsymbol{r}), \tag{2}$$

where $\varphi_i(\boldsymbol{r})$ is the ith mode eigenfunction and a_i is the expansion coefficient of the ith mode. Using this initial fission source distribution, the fission source distribution in the next cycle is obtained by applying operator **A**, which corresponds to one cycle of power iteration, to drive the fission source distribution to the next cycle as follows:

$$F_1(\boldsymbol{r}) = \mathbf{A}F_0(\boldsymbol{r}) = \sum_{i=0}^{\infty} a_i \mathbf{A}\varphi_i(\boldsymbol{r}) = \sum_{i=0}^{\infty} a_i k_i \varphi_i(\boldsymbol{r}), \tag{3}$$

where k_i is the ith mode eigenvalue. The eigenvalues are ordered in a descending sequence as $k_0 > k_1 \geq k_2, \ldots, > 0$, and thus, the largest eigenvalue k_0 is equal to k_{eff}. After this procedure is repeated *n* times, the fission source distribution is expressed as follows:

$$F_{\mathrm{n}}(\boldsymbol{r}) = \mathbf{A}^{\mathrm{n}} F_0(\boldsymbol{r}) = k_0^n a_0 \varphi_0(\boldsymbol{r}) + k_0^n \sum_{i=1}^{\infty} a_i \rho_i^n \varphi_i(\boldsymbol{r}), \tag{4}$$

where $\rho_i = (k_i/k_0)$. $\rho_i(< 1)$ in Eq. (4) represents the attenuation rate of the ith eigenmode.

The largest attenuation rate is the dominance ratio $\rho_1 = (k_1/k_0)$, which dominates the convergence rate and stability of the fission source distribution. Assuming that k_0 has already been determined by performing the *k*-eigenvalue calculation, we obtain the following by dividing $F_{\mathrm{n}}(\boldsymbol{r})$ by k_0^n:

$$G_n(\boldsymbol{r}) \equiv \frac{1}{k_0^n} F_{\mathrm{n}}(\boldsymbol{r}) = a_0 \rho_0^n \varphi_0(\boldsymbol{r}) + \sum_{i=1}^{\infty} a_i \rho_i^n \varphi_i(\boldsymbol{r}), \tag{5}$$

where

$$\rho_0^n = \left(\frac{k_0}{k_0}\right)^n = 1. \tag{6}$$

Thus, the first term on the right-hand side of Eq. (5) has a constant value throughout the cycles. After the power iteration is performed many times, $G_n(\boldsymbol{r})$ eventually converges to a constant value as follows:

$$\lim_{n\to\infty} G_n(\boldsymbol{r}) = a_0 \varphi_0(\boldsymbol{r}), \tag{7}$$

because $\rho_i < 1$ for $i \geq 1$. Applying an appropriate numerical reduction algorithm such as DMD to the transient state of $G_n(\boldsymbol{r})$ before convergence yields ρ_i and $\varphi_i(\boldsymbol{r})$ for several lower-order eigenmodes.

In deterministic power iteration methods such as the finite difference method, a pointwise fission source is assigned to each mesh point. In contrast, in the Monte Carlo power iteration method, the fission source is averaged over a tally region that has a finite volume, and statistical noise is involved. Hence, the fission source that is calculated with the Monte Carlo method does not truly represent the pointwise fission source distribution $G_n(\boldsymbol{r})$. With the Monte Carlo method, a dilemma is encountered: the finer the tally region is, the larger the statistical noise of each tally becomes.

This section presents a Monte Carlo algorithm for calculating samples of the fission source distribution in each cycle for use as snapshots for DMD analysis. The Monte Carlo *k*-eigenvalue calculation for dominance ratio assessment is performed via the following steps.

1) Before starting the Monte Carlo power iterations for snapshots of DMD, a *k*-eigenvalue calculation is performed to obtain k_{eff} (k_0). This should be calculated precisely using a sufficient number of histories because it will be used in the following steps. The accuracy of k_{eff} directly affects the dominance ratio that is calculated with the DMD method. How precisely k_{eff} should be calculated depends on the target accuracy of the dominance ratio. If the dominance ratio needs to be calculated up to four digits, the statistical uncertainty of k_{eff} should be much less than 10 pcm.
2) A *k*-eigenvalue calculation is initiated for the snapshots. In the first cycle, *N* initial fission sources are allocated within the calculation domain. The fission source distribution can be arbitrarily determined; however, the distribution needs to include the first eigenmode, $\varphi_1(\boldsymbol{r})$, to assess the dominance ratio. For instance, a point source that is located at the node of the first eigenmode should be avoided.
3) The fissioning region is discretized into tally regions where fission sources accumulate. The number of tally regions and their sizes can be arbitrarily determined. Suitable determination of the tally regions will be discussed in the numerical tests in Section 4.
4) The standard random walk process for *k*-eigenvalue calculation, where forced fission and implicit capture are used, is performed until all initial *N* fission sources are killed by Russian

roulette or escape from the external boundary. The fission source is calculated in the ith tally region as follows:

$$x_{i,1} = \frac{1}{k_{eff}} \sum_k \frac{\nu\Sigma_f}{\Sigma_t} w_k, \tag{8}$$

where the summation is performed over all collisions in the ith tally region during the first cycle; k denotes the kth collision; w_k is the particle weight at the kth collision; $\nu\Sigma_f$ and Σ_t are the production cross section and total cross section, respectively, in the ith tally region; and k_{eff} is the value that was calculated in Step 1. This fission source is not used as the fission source in the next cycle. The fission sources for the next cycle are separately determined by following the manner widely used in Monte Carlo codes. The fission source can also be calculated with the track length estimator as follows:

$$x_{i,1} = \frac{1}{k_{eff}} \sum_k \nu\Sigma_f s_k w_k, \tag{9}$$

where the summation is performed over tracks in the ith tally region during the first cycle, k denotes the kth track, and s_k is the kth track length.

5) In the next cycle, the fission sources start from the fission source sites that were determined in the previous cycle. Usually, Monte Carlo k-eigenvalue calculations are performed with an almost constant number of fission neutrons in each cycle. For this purpose, the weight of each starting particle is N/M, where M (which varies among cycles) is the number of source particles that was determined in the previous cycle. This normalization needs to be canceled out when calculating the fission source, $G_n(\boldsymbol{r})$, which is defined in Eq. (5). Thus, the fission source in the ith tally region in the jth cycle ($j \geq 2$) is calculated as follows:

$$x_{i,j} = \frac{1}{k_{eff}} \frac{M}{N} \sum_k \frac{\nu\Sigma_f}{\Sigma_t} w_k \quad \text{for the collision estimator,} \tag{10}$$

$$x_{i,j} = \frac{1}{k_{eff}} \frac{M}{N} \sum_k \nu\Sigma_f s_k w_k \quad \text{for the track length estimator.} \tag{11}$$

6) In an ordinary Monte Carlo calculation for the k-eigenvalue, the power iteration is continued to calculate k_{eff} with a desired level of confidence even after the fission source distribution

has fully converged to the fundamental mode. However, the number of times that the power iteration for dominance ratio assessment should be performed is one of the subjects of this study, and it is discussed in Section 4.

3. DMD for dominance ratio assessment

This section describes the DMD method for assessing the dominance ratio using the transition state of the fission source toward the fundamental mode distribution. DMD has been presented in detail in many studies. An outline of DMD that focuses on its application to dominance ratio assessment is briefly presented here. The DMD algorithm that is used in this study is based on the description in Chapter 1 in (Kutz et al., 2016), which is partially the same as that used in (Yamamoto and Sakamoto, 2021) and (Yamamoto and Sakamoto, 2022). For more details, readers can refer to previous publications such as (Kutz et al., 2016). However, to facilitate reading, the concise overview of the DMD based on the presentation in (Kutz et al., 2016) is given here.

Let us assume that fission sources are obtained in *n* tally regions from the 1st to the *J*th cycle according to the procedure that is presented in Section 2. An *n*-dimensional column vector that is composed of the set of *n* fission sources in the *k*th cycle ($1 \le k \le J$) is constructed as follows:

$$\mathbf{x}_k = \left[x_{1,k} \ \ x_{2,k} \dots x_{i,k} \dots x_{n,k}\right]^T, \tag{12}$$

where $x_{i,k}$ is the fission source of the *i*th tally region in the *k*th cycle. Each $\mathbf{x}_k$ corresponds to a snapshot in the dynamic mode. Using $\mathbf{x}_k$ for $k = 1, \dots, J$, two matrices, $\mathbf{X}$ and $\mathbf{X}'$, are constructed as follows:

$$\mathbf{X} = \left[\mathbf{x}_1 \ \ \mathbf{x}_2 \dots \mathbf{x}_j \dots \mathbf{x}_{J-1}\right], \tag{13}$$

$$\mathbf{X}' = \left[\mathbf{x}_2 \ \ \mathbf{x}_3 \dots \mathbf{x}_j \dots \mathbf{x}_J\right]. \tag{14}$$

The dimensions of $\mathbf{X}$ and $\mathbf{X}'$ are both $n \times (J-1)$. The two matrices are related as follows: $\mathbf{X}_{\mathrm{i,j+1}} = \mathbf{X}'_{\mathrm{i,j}}$ for $i = 1, \dots, n$ and $j = 1, \dots, J-1$.

By assuming a locally linear approximation and introducing a linear operator matrix $\mathbf{A}'$, $\mathbf{X}$ is approximately forward iterated to $\mathbf{X}'$ by one cycle as follows:

$$\mathbf{X}' \approx \mathbf{A}'\mathbf{X}. \tag{15}$$

The matrix $\mathbf{A}'$ is a discrete form of the operator $\mathbf{A}$ used in Eq. (3). The best-fit matrix for $\mathbf{A}'$ is expressed as follows:

$$\mathbf{A}' = \mathbf{X}'\mathbf{X}^{\dagger}, \tag{16}$$

where $\dagger$ denotes the Moore−Penrose pseudoinverse (Penrose, 1955) and the dimensions of $\mathbf{A}'$ are $n \times n$.

First, singular value decomposition of $\mathbf{X}$ is performed as follows:

$$\mathbf{X} = \mathbf{U}\boldsymbol{\Sigma}\mathbf{V}^{*}, \tag{17}$$

where the asterisk $*$ denotes the conjugate transpose. The dimensions of $\mathbf{U}, \boldsymbol{\Sigma}$, and $\mathbf{V}$ are $n \times n$, $n \times n$, and $(J-1) \times n$, respectively. The columns of $\mathbf{U}$ and $\mathbf{V}$ are called the left and right singular vectors, respectively, of $\mathbf{X}$. The matrix $\boldsymbol{\Sigma}$ consists of singular values on its diagonal.

Since the fission sources are calculated with the Monte Carlo method, each component of the matrix $\mathbf{X}$ involves statistical noise. A contentious issue in the DMD algorithm is the sensitivity of the results to the noise in each element $x_{i,k}$ of the data matrix $\mathbf{X}$. DMD results are biased by including too many modes that correspond to small singular values. A simple way to denoise or debias is to truncate low-energy modes. An appropriate low-rank truncation to $\mathbf{U}$, $\boldsymbol{\Sigma}$, and $\mathbf{V}$ could yield optimal solutions. However, it is challenging to decide how many singular values are retained. This issue has been discussed in many publications (e.g., Chapter 8 in (Kutz et al., 2016), (Dawson et al., 2016)).

Once a low rank r $(\leq \min(n, J-1))$ has been determined via a reasonable strategy, $\mathbf{X}$ is approximated by the truncated matrices:

$$\mathbf{X} \approx \mathbf{U}_{\mathrm{r}}\boldsymbol{\Sigma}_{\mathrm{r}}\mathbf{V}_{\mathrm{r}}^{*}, \tag{18}$$

where $\mathbf{U}_{\mathrm{r}} \in \mathbb{C}^{\mathrm{n}\times\mathrm{r}}, \boldsymbol{\Sigma}_{\mathrm{r}} \in \mathbb{C}^{\mathrm{r}\times\mathrm{r}}$, and $\mathbf{V}_{\mathrm{r}} \in \mathbb{C}^{(\mathrm{J}-1)\times\mathrm{r}}$. The pseudoinverse of $\mathbf{X}$ is expressed as follows:

$$\mathbf{X}^{\dagger} = \mathbf{V}_{\mathrm{r}}\boldsymbol{\Sigma}_{\mathrm{r}}^{-1}\mathbf{U}_{\mathrm{r}}^{*}. \tag{19}$$

Rank reduction of matrix $\mathbf{A}'$ from $n \times n$ to $r \times r$ is performed as follows:

$$\widetilde{\mathbf{A}'} = \mathbf{U}_{\mathrm{r}}^{*}\mathbf{A}'\,\mathbf{U}_{\mathrm{r}} = \mathbf{U}_{\mathrm{r}}^{*}\mathbf{X}'\mathbf{X}^{\dagger}\mathbf{U}_{\mathrm{r}} = \mathbf{U}_{\mathrm{r}}^{*}\mathbf{X}'\mathbf{V}_{\mathrm{r}}\boldsymbol{\Sigma}^{-1}. \tag{20}$$

The transformation from $\mathbf{A}'$ to $\widetilde{\mathbf{A}'}$ is a similarity transformation, and the two matrices share the same eigenvalues. Applying the eigendecomposition to $\widetilde{\mathbf{A}'}$ yields

$$\widetilde{\mathbf{A}'}\mathbf{W} = \mathbf{W}\mathbf{P}, \tag{21}$$

where the columns of $\mathbf{W}$ are eigenvectors and $\mathbf{P}$ is a diagonal matrix that contains the corresponding eigenvalues ρ_m $(0 \leq m \leq r-1)$.

The largest real-valued eigenvalue ρ_0 corresponds to ρ_0 in Eq. (5) and it is supposed to be unity. The dominance ratio is equal to the second-largest real-valued eigenvalue ρ_1. The diagonal components of $\mathbf{P}$ are also the eigenvalues of $\mathbf{A}'$. The eigenvectors of $\mathbf{A}'$ are expressed by the columns of $\mathbf{\Phi}$:

$$\mathbf{\Phi} = \mathbf{X}'\mathbf{V}_\mathrm{r}\mathbf{\Sigma}_\mathrm{r}^{-1}\mathbf{W}. \tag{22}$$

Using the eigenvalues and eigenvectors of $\mathbf{A}'$, snapshots of the fission source as a function of the cycle *k* are reconstructed as follows:

$$\mathbf{x}(k) \approx \mathbf{\Phi}\mathbf{P}^{k-1}\mathbf{b}, \tag{23}$$

where

$$\mathbf{b} = [b_0\ b_1\ \dots\ b_m\ \dots\ b_{r-1}\ ]^T, \tag{24}$$

b_m is the amplitude of the *m*th mode for the first cycle $k = 1$. Since $\mathbf{x}_1 = \mathbf{x}(1) = \mathbf{\Phi}\mathbf{b}$, the amplitude vector of the first cycle is expressed as follows:

$$\mathbf{b} = \mathbf{\Phi}^\dagger\mathbf{x}_1, \tag{25}$$

where $\mathbf{\Phi}^\dagger$ is the Moore–Penrose pseudoinverse of $\mathbf{\Phi}$.

4. Application of DMD to dominance ratio assessment

4.1 Model description

As numerical tests of the proposed Monte Carlo method, *k*-eigenvalue calculations for dominance ratio assessment using DMD were performed for a three-dimensional rectangular geometry in which two fuel slabs were separated by a 700 ppm borated light-water isolator. Each fuel slab was composed of a homogenized low-enriched UO_2 fuel rod array. The calculation model that was used for the numerical tests is illustrated in Fig. 1. The dimensions in Fig. 1 are listed in Table 1.

The calculations were performed using the 3-energy group constants, as presented in Tables 2 and 3. The group constants were prepared using the standard reactor analysis code (SRAC) (Okumura et al., 2007). Anisotropic scattering was considered up to the P_1 order. The scattering cross sections that are not listed in the tables were all zero.

In Cases 1 and 3, each calculation model was symmetric with respect to the *y*-*z* plane at the center of the light-water isolator. Cases 2 and 4 were composed of the left fuel slab only, namely, they corresponded to a single fissioning material. Vacuum boundary conditions were imposed on the external boundaries.

The calculations were performed using an in-house Monte Carlo code that was developed by the authors. For reference solutions of the dominance ratios, the fundamental mode *k*-eigenvalue k_{eff} and the 1st mode *k*-eigenvalue were calculated for each case. A Monte Carlo method (MPM) that was proposed by Booth (2003) and Yamamoto (2009) was used to calculate the 1st mode *k*-eigenvalue. The criticality calculations for k_{eff} and the 1st mode *k*-eigenvalue were performed with 1,200 active cycles, 500,000 neutrons per cycle, and 40 inactive cycles. The inactive cycles were enough for the eigenvalue convergence even though they were not enough for the fission source convergence.

Case 1, in which the dominance ratio was 0.907, was a moderate example in terms of fission source convergence, which may often occur in *k*-eigenvalue calculations.

Case 2, in which the dominance ratio was 0.721, was a tightly coupled system due to its small size (45 cm × 40 cm × 35 cm). The dominance ratio of Case 2 was relatively low, which caused the fission source to converge rapidly.

Case 3, in which the two fuel slabs were separated by a 28 cm-thick isolator, was a loosely coupled system. The dominance ratio in Case 3 was 0.9992, and the fission source distribution changed very slightly in each power iteration.

Case 4 also had a high dominance ratio of 0.996, which was caused by the large dimensions (600 cm × 500 cm × 450 cm). Cases 3 and 4 were extreme examples of slow fission source convergence.

Table 1 Dimensions and dominance ratios of the numerical tests

Case	X_1 (cm)	W (cm)	X_2 (cm)	Y (cm)	Z (cm)	Dominance ratio ρ
1	30	6	30	60	50	0.90673 ± 0.00005
2	45	0	0	40	35	0.72128 ± 0.00005
3	30	28	30	60	50	0.99915 ± 0.00004
4	600	0	0	500	450	0.99588 ± 0.00002

Table 2 Three group constants of the homogenized UO_2 fuel rod array

	1st group (10 MeV~67 keV)	2nd group (67 keV~0.993 eV)	3rd group (0.993 eV~)
Σ_t (cm^{-1})	3.22058E-1*	1.01682	1.72854
Σ_c (cm^{-1})	5.75842E-4	1.350145E-2	3.067833E-2
$\nu\Sigma_f (\mathrm{cm}^{-1})$	5.25926E-3	7.81332E-3	7.36280E-2
$\Sigma_{s0g\to g}$ (cm^{-1})**	2.61779E-1	9.39127E-1	2.5313E+0
$\Sigma_{s1g\to g}$ (cm^{-1})***	1.93300E-1	5.05296E-1	7.99853E-1
$\Sigma_{s0g\to g+1}$ (cm^{-1})**	5.75119E-2	6.09358E-2	—
$\Sigma_{s1g\to g+1}$ (cm^{-1})***	1.25967E-2	2.54734E-2	—
χ_g	0.993338	6.662E-3	0

*Read as 3.22058×10^{-1}, **P_0 component, ***P_1 component

Table 3 Three group constants of 700 ppm borated water

	1st group (10 MeV~67 keV)	2nd group (67 keV~0.993 eV)	3rd group (0.993 eV~)
Σ_t (cm^{-1})	4.07673E-1*	1.38975	2.67852
Σ_c (cm^{-1})	2.25214E-4	1.47193E-3	4.13576E-2
$\Sigma_{s0g\to g}$ (cm^{-1})**	3.13425E-1	1.26381	2.63724
$\Sigma_{s1g\to g}$ (cm^{-1})***	2.41867E-1	8.47353E-1	1.12044
$\Sigma_{s0g\to g+1}$ (cm^{-1})**	9.40222E-2	1.24472E-1	—
$\Sigma_{s1g\to g+1}$ (cm^{-1})***	2.57208E-2	4.32277E-2	—

*Read as 4.07673×10^{-1}, **P_0 component, ***P_1 component

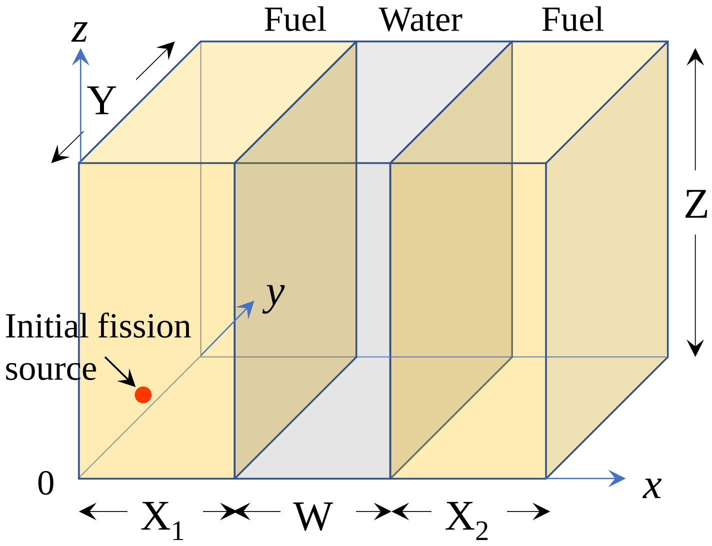

Fig. 1 Geometry for the numerical tests for Cases 1 and 3

An isotropic point fission source was positioned at $x = (X_1 + X_2)/5$, $y = Y/5$, and $z = z/5$ as an initial fission source, namely, the initial source neutrons were emitted from the left slab only. This position was intentionally chosen to excite higher eigenmodes, including the 1st eigenmode. The entire fissioning region was equally divided into 12 × 12 × 12 regions, each of which was a tally region of fission sources, as defined by Eq. (10). In Cases 1 and 3, the left and right slabs were equally divided into 6 × 12 × 12 tally regions each. By combining the results of adjacent 2 × 2 × 2 regions, 3 × 3 × 3 regions, and 6 × 6 × 6 regions, we obtained the results of the fission source for 6 × 6 × 6 regions, 4 × 4 × 4 regions, and 2 × 2 × 2 regions, respectively. The number of initial fission source neutrons was N =12,000,000. Throughout the subsequent cycles, the product of the number of fission source neutrons and the particles' initial weight was maintained at N by adjusting the weight of the starting particles.

4.2 Results for Case 1 ($\rho \approx 0.907$)

The initial fission source was positioned at $x = 12$ cm, $y = 12$ cm, and $z = 10$ cm. Power iterations were performed up to the 100th cycle. The fission source convergence at two positions is shown in Fig. 2. One is the initial source position, where the fission source decreased very sharply with the iterations. The other is the upper-rightmost position in Fig. 1, namely, the most remote position from the initial source, where the fission source converged the most slowly. As shown in Fig. 2, the fission source converged far before the last cycle, namely, the 100th cycle.

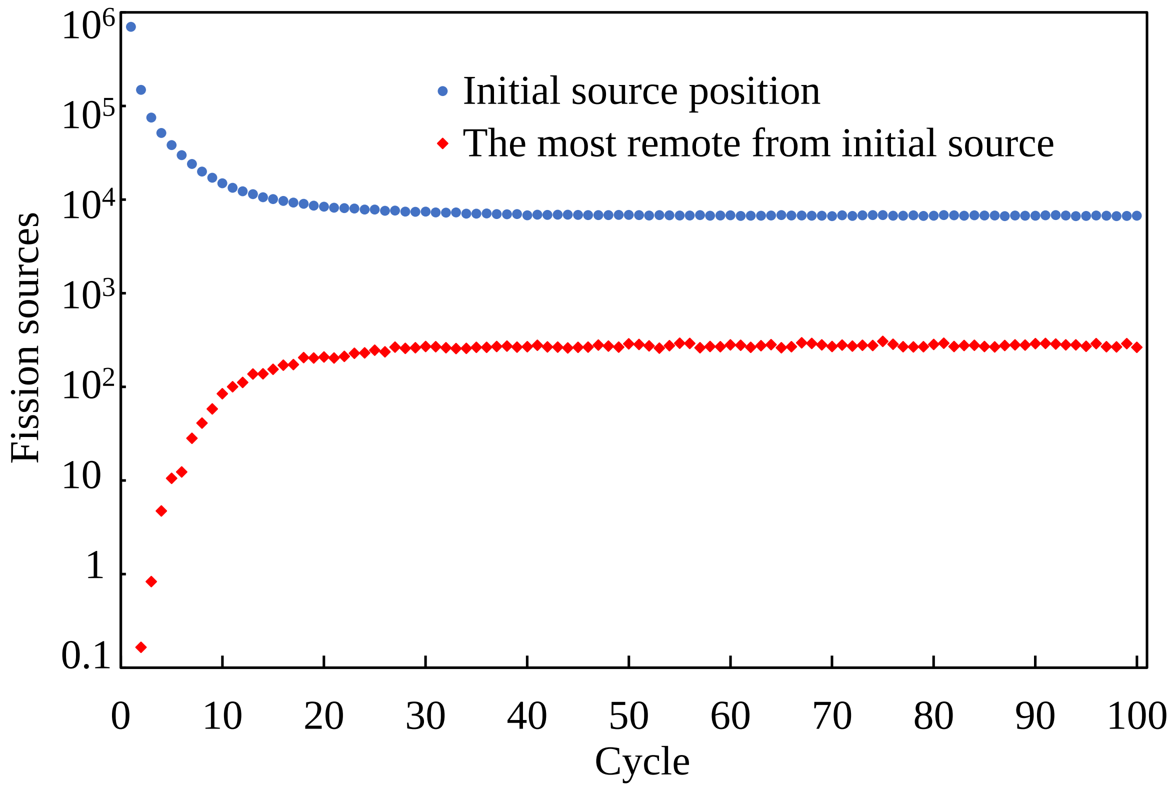

Fig. 2 Fission source convergence in Case 1

During the course of the power iterations, a data matrix that was composed of 1728 (= 12 × 12 × 12) rows and 100 snapshots (100 columns) was calculated for application to DMD analyses. However, it was not necessary to use all snapshots for the dominance ratio assessment. Since the first several snapshots may have been largely influenced by higher eigenmodes beyond the 1st mode, truncating them in the DMD analyses was expected to yield a better result.

Fig. 2 suggests that using the snapshots after convergence (beyond the ~40th cycle) would not contribute to further improvement. As stated in Section 3, the rank r needs to be suitably chosen to truncate small unnecessary singular values. The DMD performance was evaluated by varying the three parameters: the rank r, initial snapshot (or cycle) I, and last snapshot (or cycle) L.

Fig. 3 shows the dominance ratio ρ vs. rank r for several initial cycles I, where the last cycle was fixed at L=100. As shown in Fig. 3, the dominance ratio ρ depended significantly on the rank r and initial cycle I. By increasing r and I gradually, the dominance ratio converged. By taking the convergence status in Fig. 3 into consideration, r = 15 and I = 4 were identified as an optimal combination. The dependences of the dominance ratio on the initial cycle I and last cycle L are shown in Figs. 4 and 5, respectively, for r =15. The initial cycle I should not be too large to avoid missing the decay of the 1st eigenmode before convergence. In this case, the initial cycle I should be less than 10. Fig. 5 indicates that the dominance ratio was almost independent of the last cycle L beyond the 40th cycle.

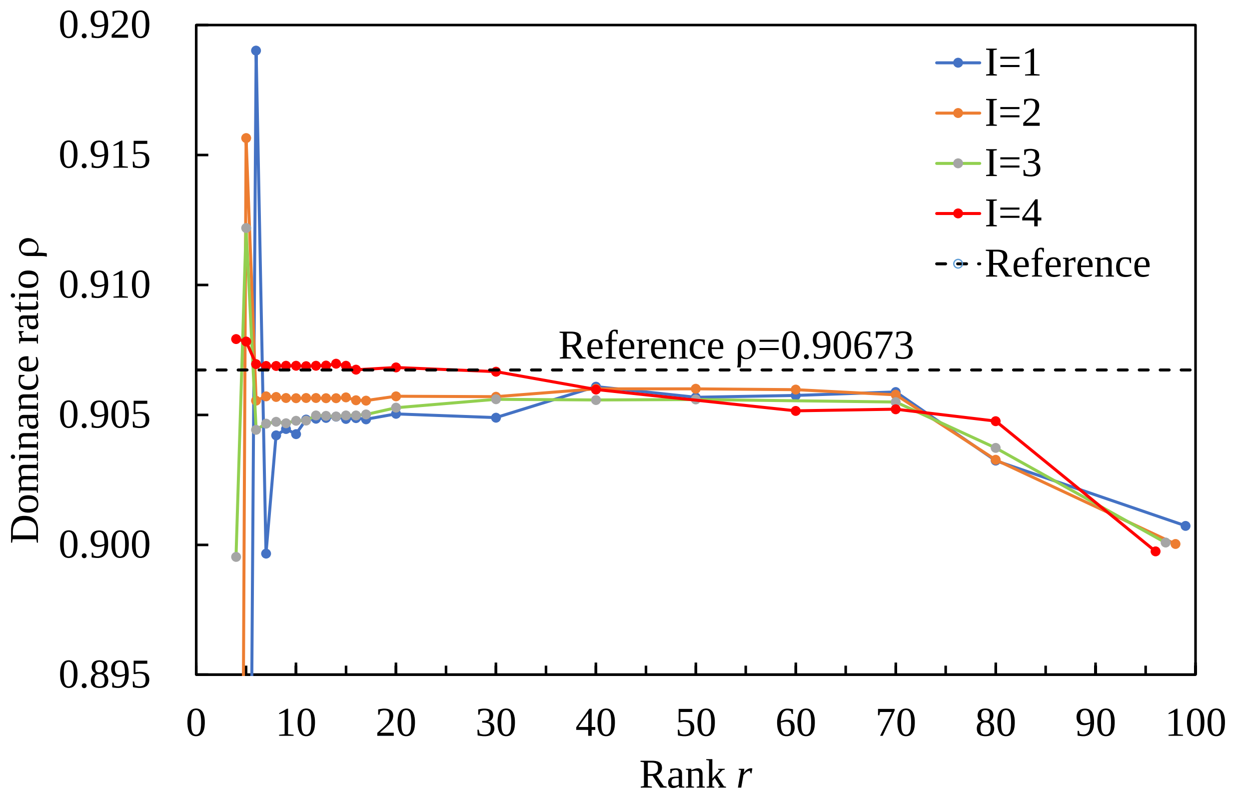

Fig. 3 Dominance ratio vs. rank r in Case 1

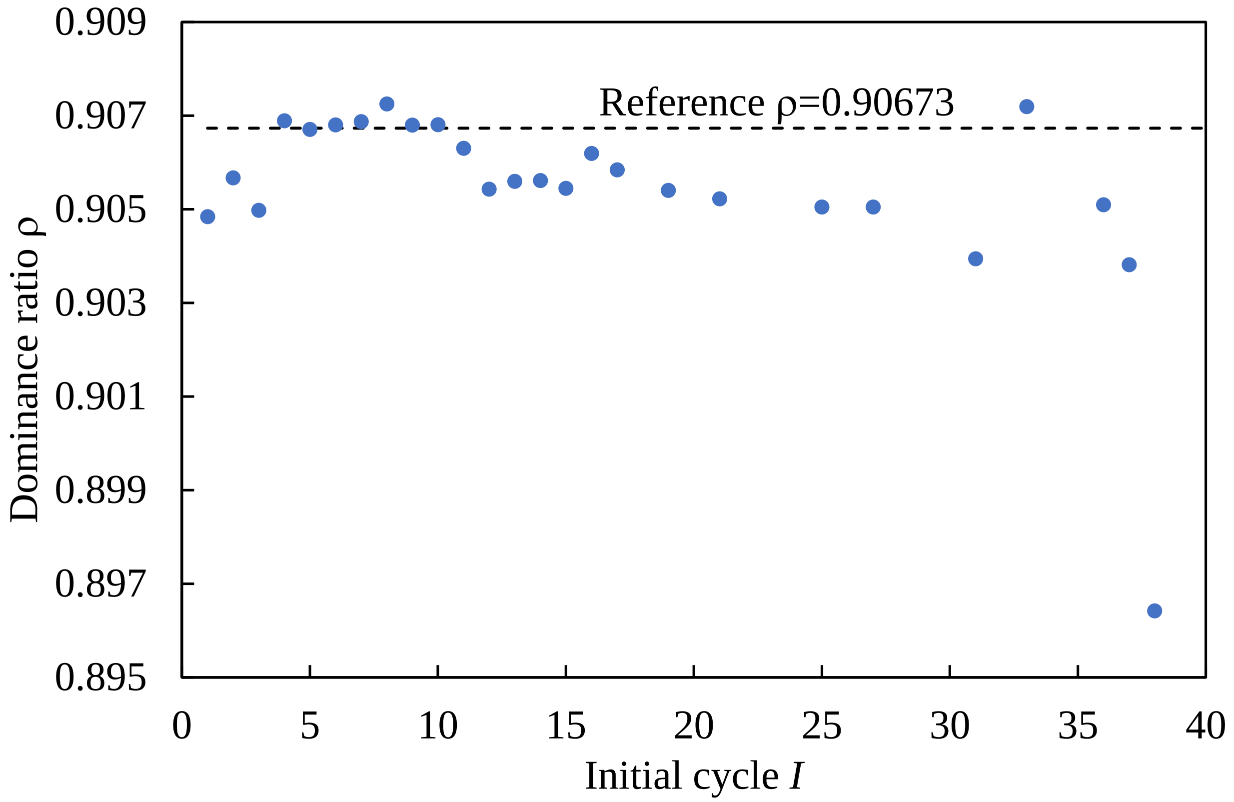

Fig. 4 Dominance ratio vs. initial cycle *I* in Case 1 (*r* = 15)

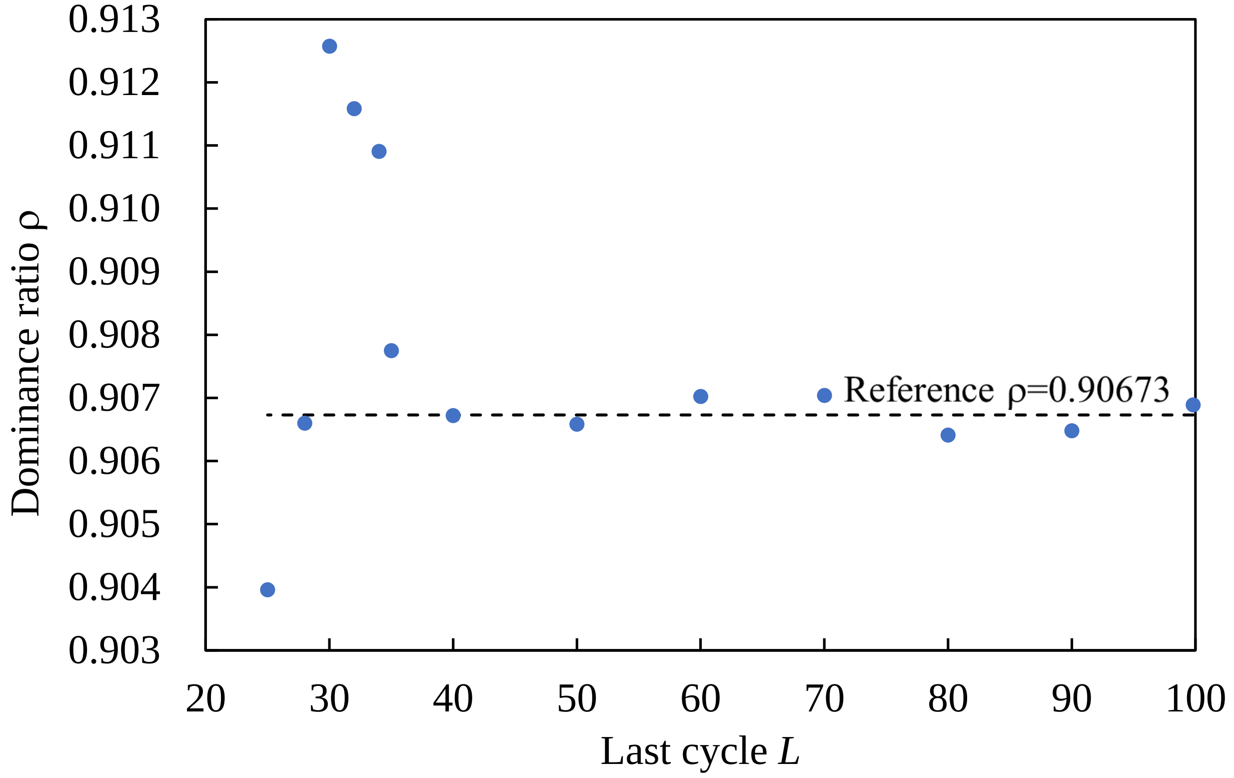

Fig. 5 Dominance ratio vs. last cycle *L* in Case 1 (*r* = 15)

The dominance ratios that were calculated for 12 × 12 × 12 regions, 6 × 6 × 6 regions, 4 × 4 × 4 regions, and 2 × 2 × 2 regions with I = 4 and L = 100 are listed in Table 4. The rank was r = 15 for the 12 × 12 × 12, 6 × 6 × 6 and 4 × 4 × 4 regions and r = 8 for the 2 × 2 × 2 regions.

The calculations for dominance ratio assessment were also performed with the FMM, and the FMM results are listed in Table 4. In general, the FMM requires sufficiently resolved spatial discretization to obtain accurate results. The finest discretization in Table 4, namely, 12 × 12 × 12, yielded an underestimated dominance ratio; hence, the discretization for the FMM was not fine enough. As easily anticipated, the dominance ratio was further underestimated as the discretization became coarser.

Table 4 Dominance ratios by DMD and the FMM

Case	Tally region	r	I	L	Dominance ratio ρ		
					DMD	Reference	FMM
1	12 × 12 × 12	15	4	100	0.90689	0.90673 ± 0.00005	0.90280
	6 × 6 × 6	15	4	100	0.90768		0.89182
	4 × 4 × 4	15	4	100	0.90703		0.88090
	2 × 2 ×2	8	4	100	0.90616		0.87634
2	12 × 12 × 12	16	3	100	0.72450	0.72128 ± 0.00005	0.71461
	6 × 6 × 6	16	3	100	0.72999		0.69459
	4 × 4 × 4	16	3	100	0.72430		0.66577
	2 × 2 ×2	8	3	100	0.73270		0.61867
3	12 × 12 × 12	30	35	700	0.99918	0.99915 ± 0.00004	0.99928
	6 × 6 × 6	30	35	700	0.99920		0.99922
	4 × 4 × 4	30	35	700	0.99920		0.99918
	2 × 2 ×2	8	25	700	0.99920		0.99921
4	12 × 12 × 12	30	30	700	0.99587	0.99588 ± 0.00002	0.98833
	6 × 6 × 6	30	30	700	0.99634		0.97805
	4 × 4 × 4	30	30	700	0.99655		0.96880
	2 × 2 ×2	8	30	700	0.99680		0.95431

In contrast, the dominance ratio that was obtained from DMD was insensitive to the number of tally regions, as presented in Table 4. The smaller the number of tally regions was, the smaller the statistical uncertainty of the fission source in each tally region was for the same particle histories because of the enlargement of each tally region. This is a favorable property for Monte

Carlo calculation for dominance ratio assessment because a coarse spatial discretization requires fewer computational resources.

The normalized fission source distributions of the fundamental mode (0th) and 1st mode in the *x* direction are shown in Fig. 6, where the results from DMD and *k*-eigenvalue calculation (reference) for 12 × 12 × 12 tally regions are compared. As shown in Fig. 6, the DMD method well reproduced the reference distributions.

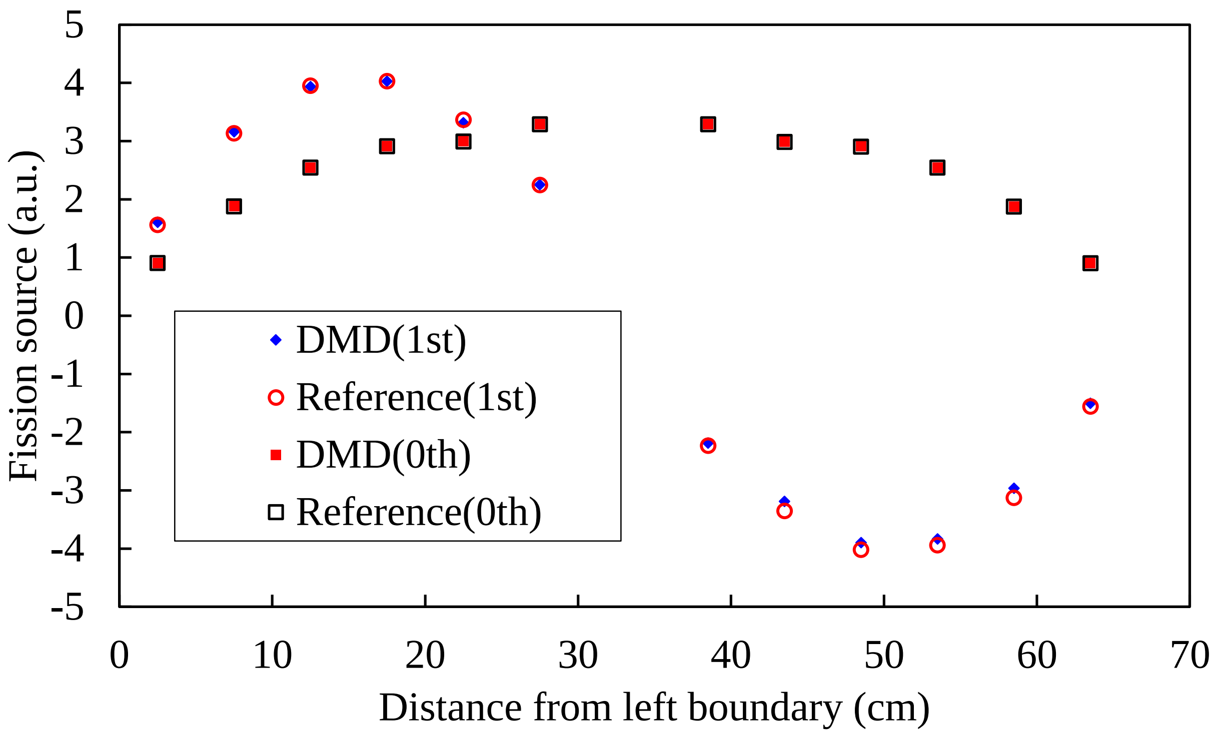

Fig.6 Normalized fission source distributions of fundamental and 1st eigenmode by DMD and eigenvalue calculation in the innermost tally region

4.3 Results for Case 2 ($\rho \approx 0.721$) (Small system)

The calculations for this tightly coupled system were performed in the same manner as in the previous case. The fission source convergence at two positions is shown in Fig. 7 for 12 × 12 × 12 tally regions. The convergence was much faster than in Case 1 because of the low dominance ratio (~ 0.721). The transition state toward convergence was only observed before the 15th cycle, beyond which the fission source maintained an almost stationary state. Thus, the number of snapshots (cycles) that were available for the DMD analyses was very limited for this low dominance ratio system, thereby suggesting that the initial cycle number I should be as low as possible so as not to miss the transition state.

Fig. 8 shows the dominance ratio ρ vs. rank r for several values of the initial cycle number I, where the last cycle was fixed at L=100. According to Fig. 8, r = 16, I = 3, and L =100 were identified as an optimal combination of the parameters. Figs. 9 and 10 show the dependence of the dominance ratio on the initial cycle I and last cycle L, respectively, for r = 16. As shown in these two figures, the dominance ratio was more sensitive to the parameters compared with the previous case. In particular, the dominance ratio was still sensitive to the last cycle L even after the fission source reached convergence (~15th cycle).

If a deceleration method that increases the number of cycles before convergence was introduced, the sensitivities of the dominance ratio with respect to the parameters for DMD analyses could be reduced, as in Case 1. The Monte Carlo Wielandt deceleration method was proposed for α-eigenvalue mode calculations (Yamamoto and Sakamoto, 2020). However, the Monte Carlo Wielandt method (Yamamoto and Miyoshi, 2004) cannot be used as a deceleration method for k-eigenvalue calculations. This is because fission sources with negative particle weights are generated and cannot be straightforwardly handled without special techniques. In conclusion, due to the reduced number of cycles before convergence in a low dominance ratio system, the dominance ratio that is obtained from the DMD method is more sensitive to the parameters. The parameters need to be suitably chosen in cases in which the fission source convergence is very fast.

The dominance ratios that were calculated for 12 × 12 × 12 regions, 6 × 6 × 6 regions, 4 × 4 × 4 regions, and 2 × 2 × 2 regions with I = 4 and L = 100 are listed in Table 4. The rank was r = 16 for the 6 × 6 × 6 and 4 × 4 × 4 regions and r = 8 for the 2 × 2 × 2 regions. Again, in contrast to the FMM, the DMD method yielded almost identical dominance ratios regardless of the number of tally regions.

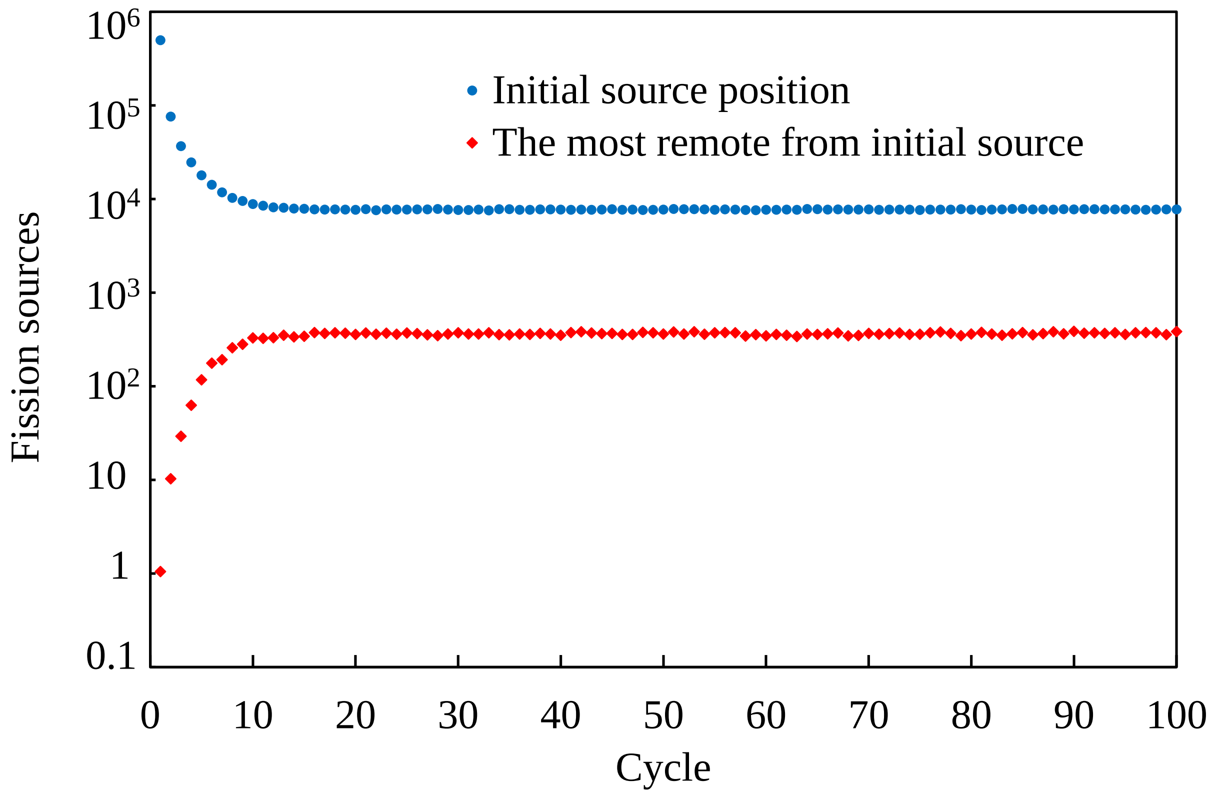

Fig. 7 Fission source convergence in Case 2

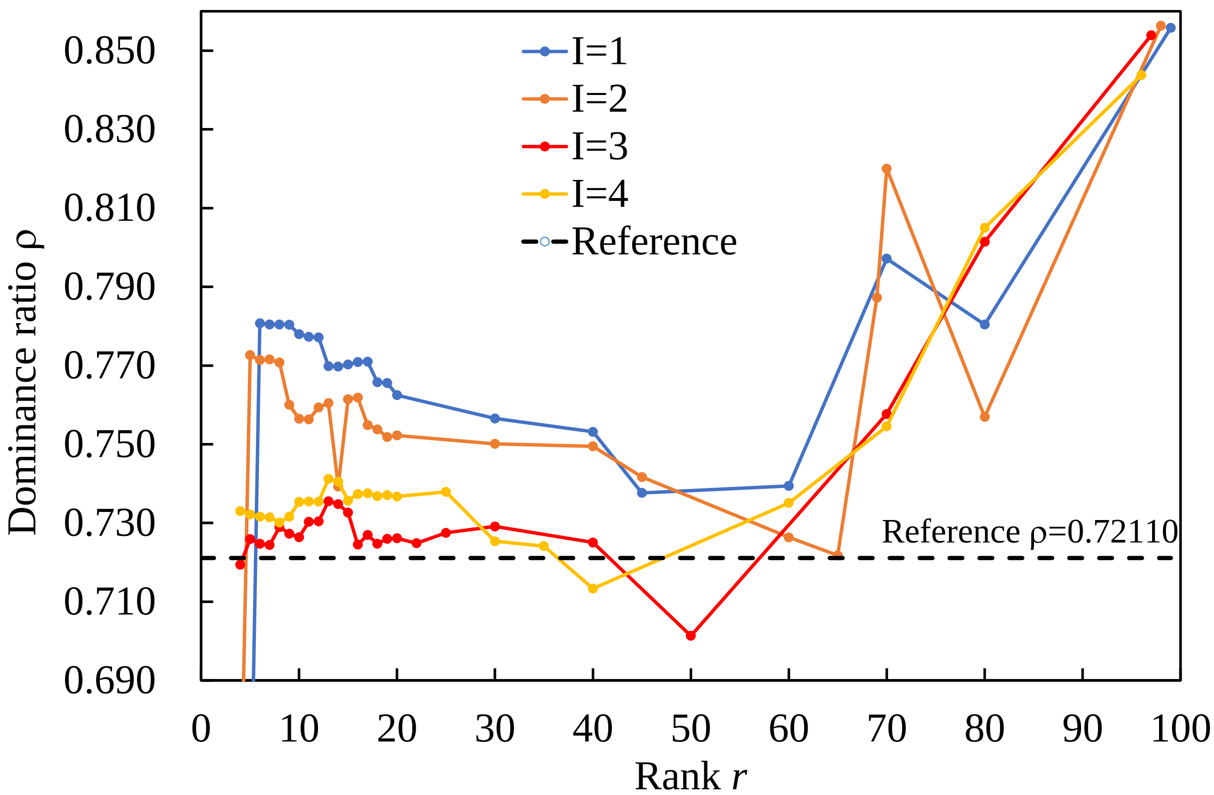

Fig. 8 Dominance ratio vs. rank r in Case 2

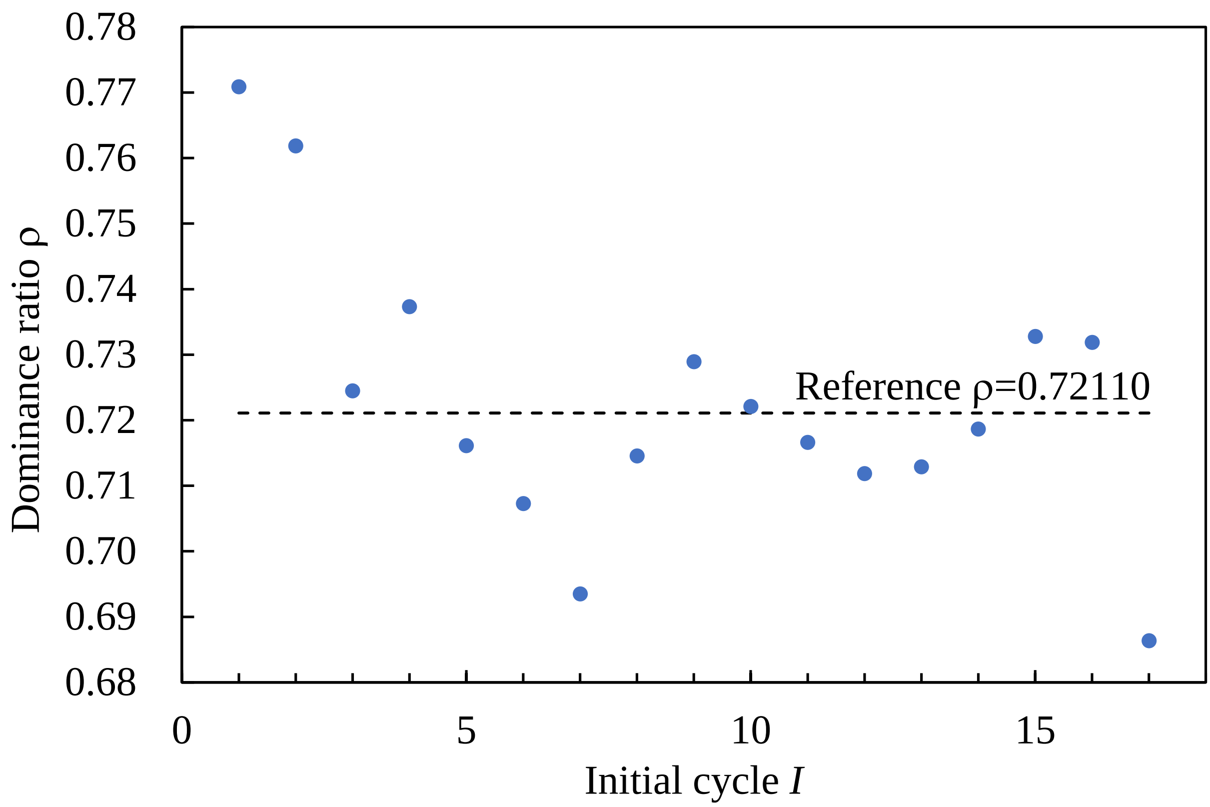

Fig. 9 Dominance ratio vs. initial cycle I in Case 2 (r = 16)

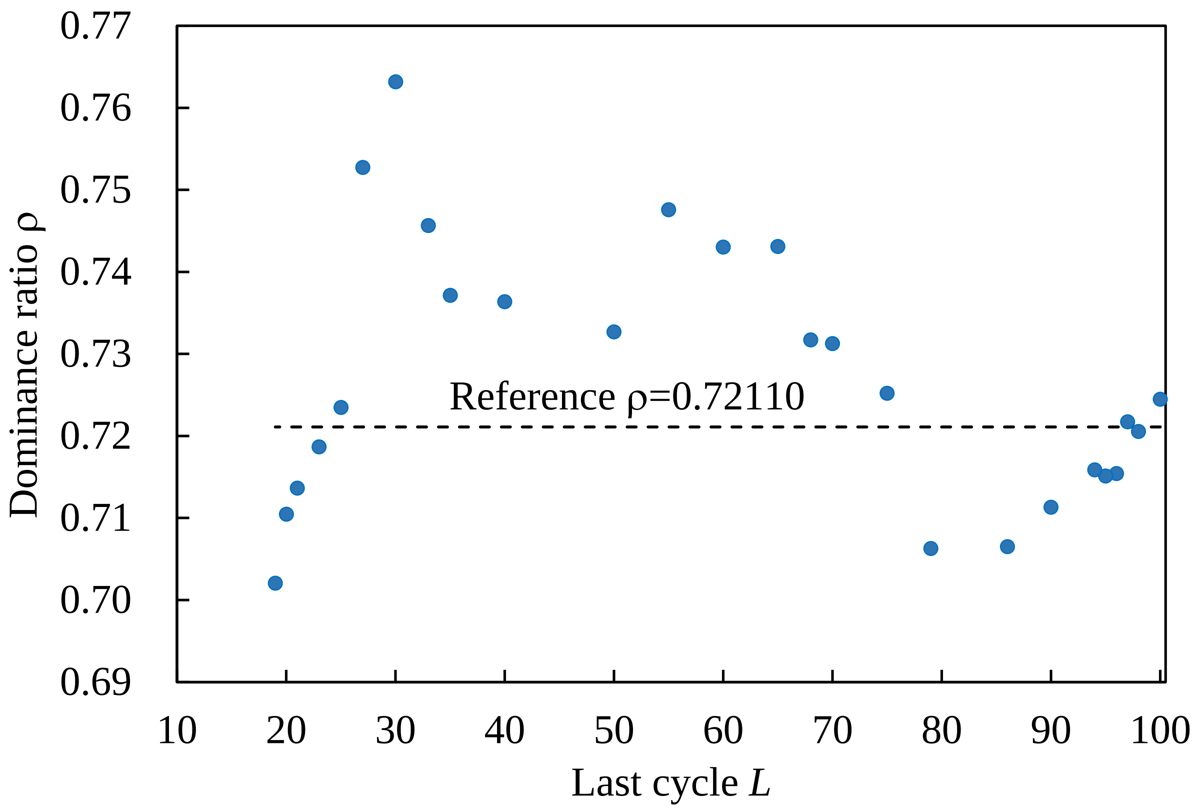

Fig. 10 Dominance ratio vs. last cycle L in Case 2 (r = 16)

4.4 Results for Case 3 ($\boldsymbol{\rho \approx 0.9992}$) (Loosely coupled two-slab system)

This example was a very loosely coupled system that was composed of two fuel slabs and a light-water isolator. The calculations were performed in the same manner as in the previous cases except that the power iterations were continued up to the 700th cycle.

The fission source convergence at two positions is shown in Fig. 11 for 12 × 12 × 12 tally regions. As shown in Fig. 11, the fission source transition at the initial source position exhibited an "elbow" around the 20th cycle and decreased very slowly beyond the elbow. The decay of the fission source beyond the elbow was mostly dominated by the 1st eigenmode. The fission source in the most remote tally region from the initial source continued to increase even after the last cycle, namely, the 700th cycle. Thus, in this high dominance ratio system, the fission source did not reach convergence by the end of the last cycle.

Fig. 12 shows the dominance ratio ρ vs. rank r for several initial cycles I, where the last cycle was fixed at L = 700. In this high dominance ratio system, the initial cycle I could be chosen to exclude higher eigenmodes than the 1st mode because $k_1 (\approx k_0)$ was significantly larger than k_2. The initial cycle was chosen to be I = 25, which was beyond the elbow. According to Fig. 12, r = 30, I = 25, and L = 700 were identified as an optimal combination of the parameters.

Figs. 13 and 14 show the dependence of the dominance ratio on the initial cycle I and last cycle L, respectively, for r = 30. As shown in these two figures, the dominance ratio was almost independent of the parameters unless an extremely large initial cycle I (> ~200th cycle) and small last cycle L (< 100th cycle) were chosen. The dominance ratios that were obtained from the DMD method for several tally regions (12 × 12 × 12, 6 × 6 × 6, 4 × 4 × 4, and 2 × 2 × 2) are listed in Table 4. The dominance ratios were almost constant regardless of the number of tally regions for this high dominance ratio system.

The dominance ratios that were obtained from the FMM precisely reproduced the reference value even for the smallest number of tally regions, 2 × 2 × 2. This is because each fuel slab was almost isolated and the fission source distribution in each fuel slab was not affected by the neutron interaction between the two fuel slabs.

Using Eq. (23), snapshots of the fission source were reconstructed for 6 × 6 × 6 tally regions. Figs. 15 and 16 show the fission source transitions that were obtained using the DMD method and *k*-eigenvalue calculation at the initial source position and the most remote position from the initial source, respectively. While the fission source that was obtained via the *k*-eigenvalue calculation fluctuated due to statistical noise, the DMD method produced good agreement with the mean value of the fluctuation.

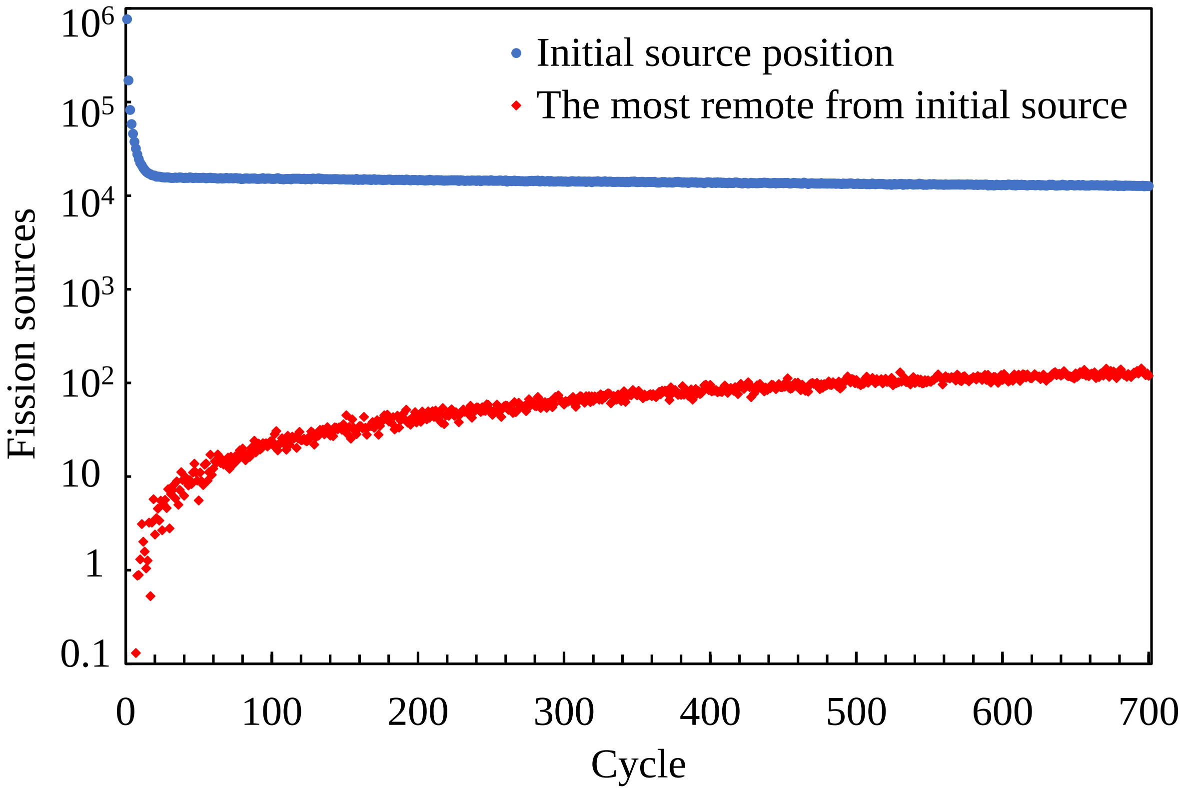

Fig. 11 Fission source convergence in Case 3

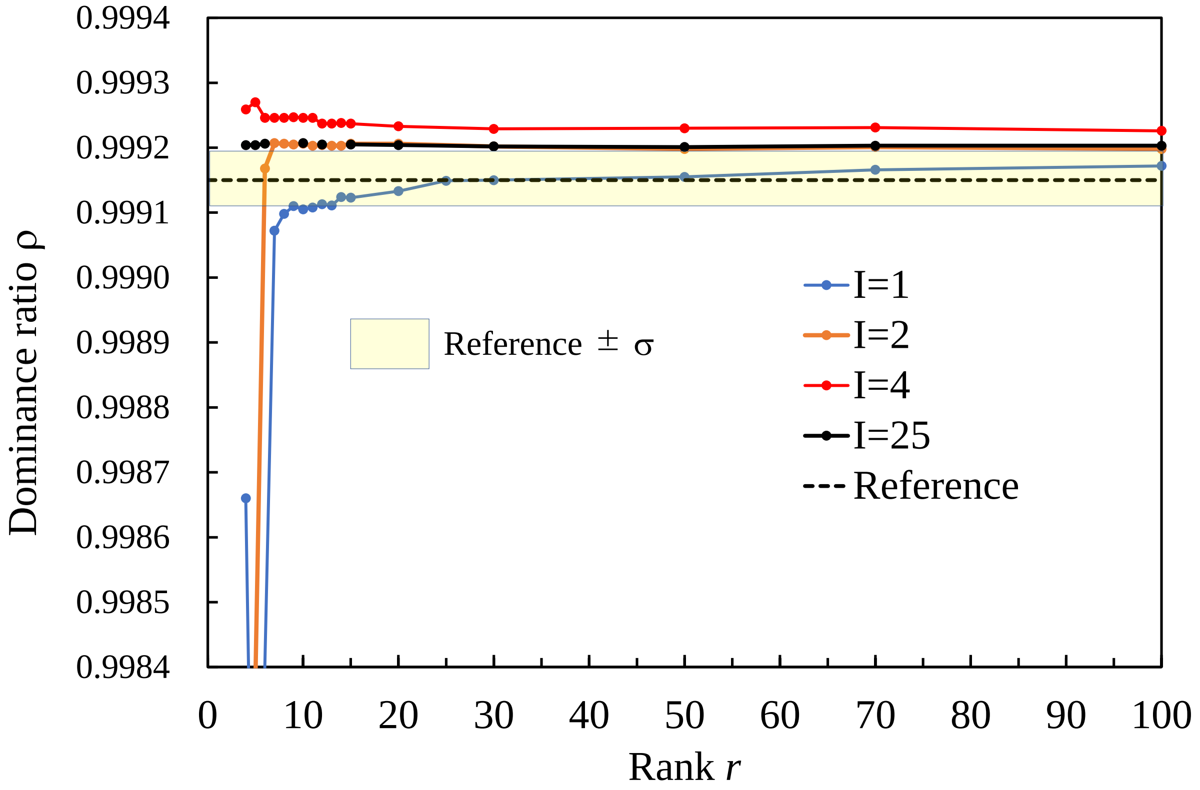

Fig. 12 Dominance ratio vs. rank *r* in Case 3

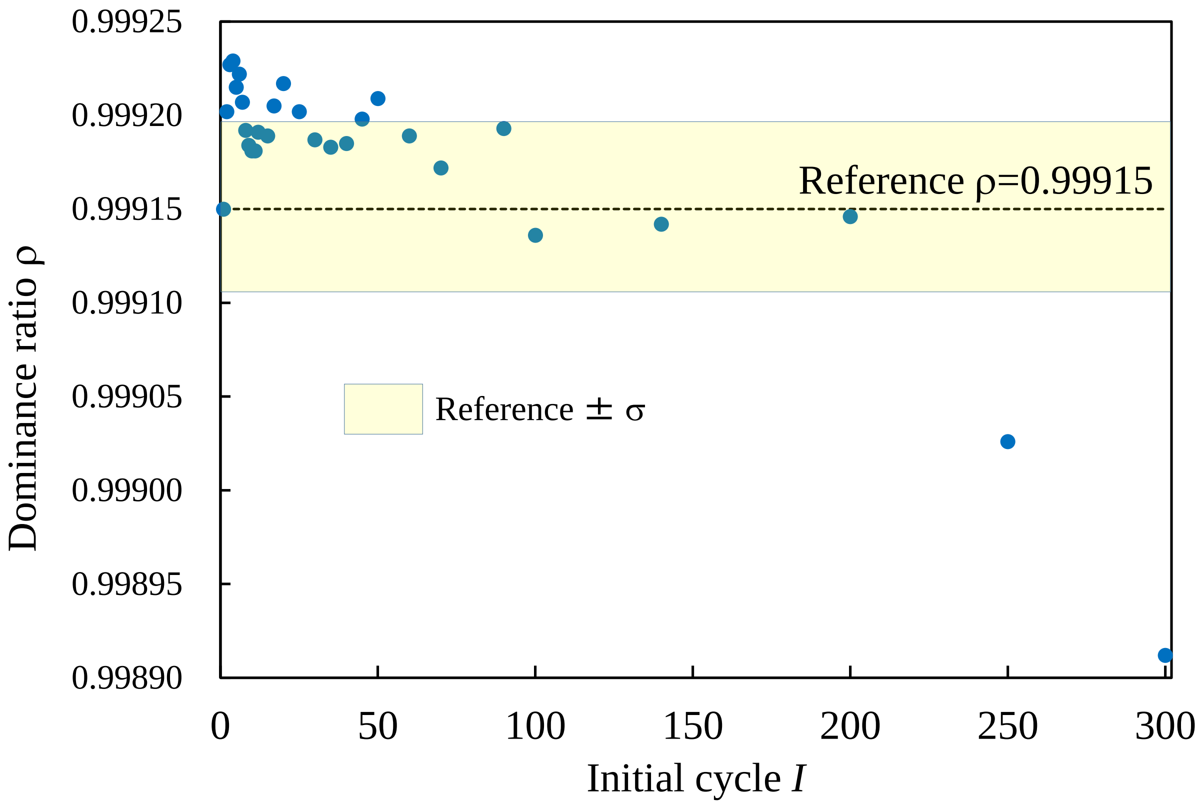

Fig. 13 Dominance ratio vs. initial cycle *I* in Case 3 (r = 30)

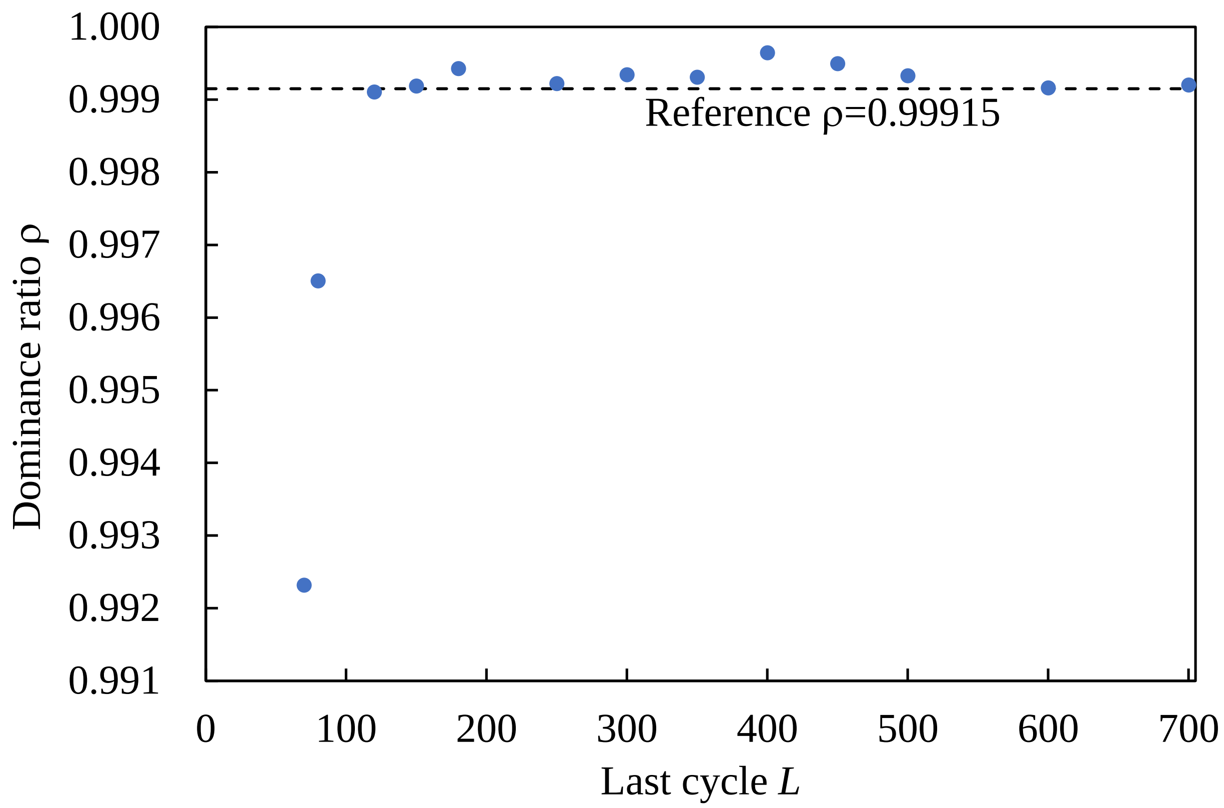

Fig. 14 Dominance ratio vs. last cycle L in Case 3 (r = 30)

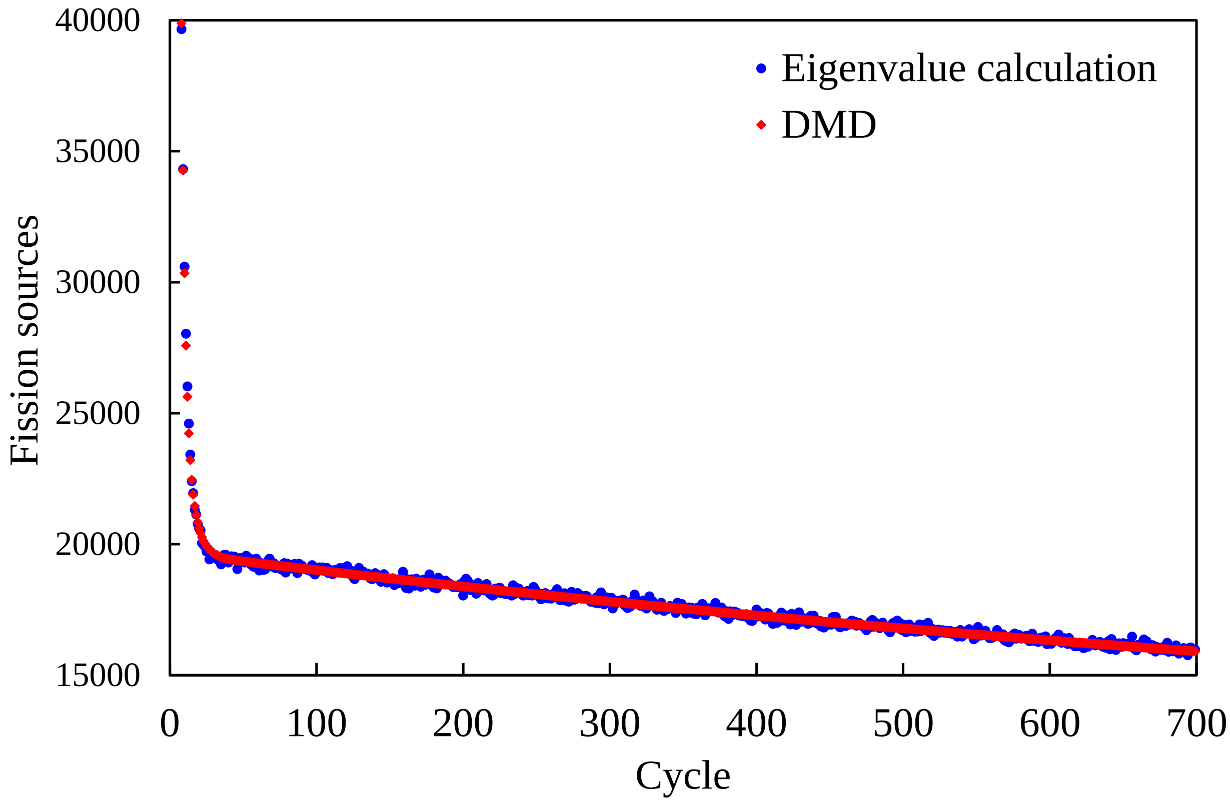

Fig. 15 Fission source transition that was reconstructed by the DMD method in Case 3 at the fission source position

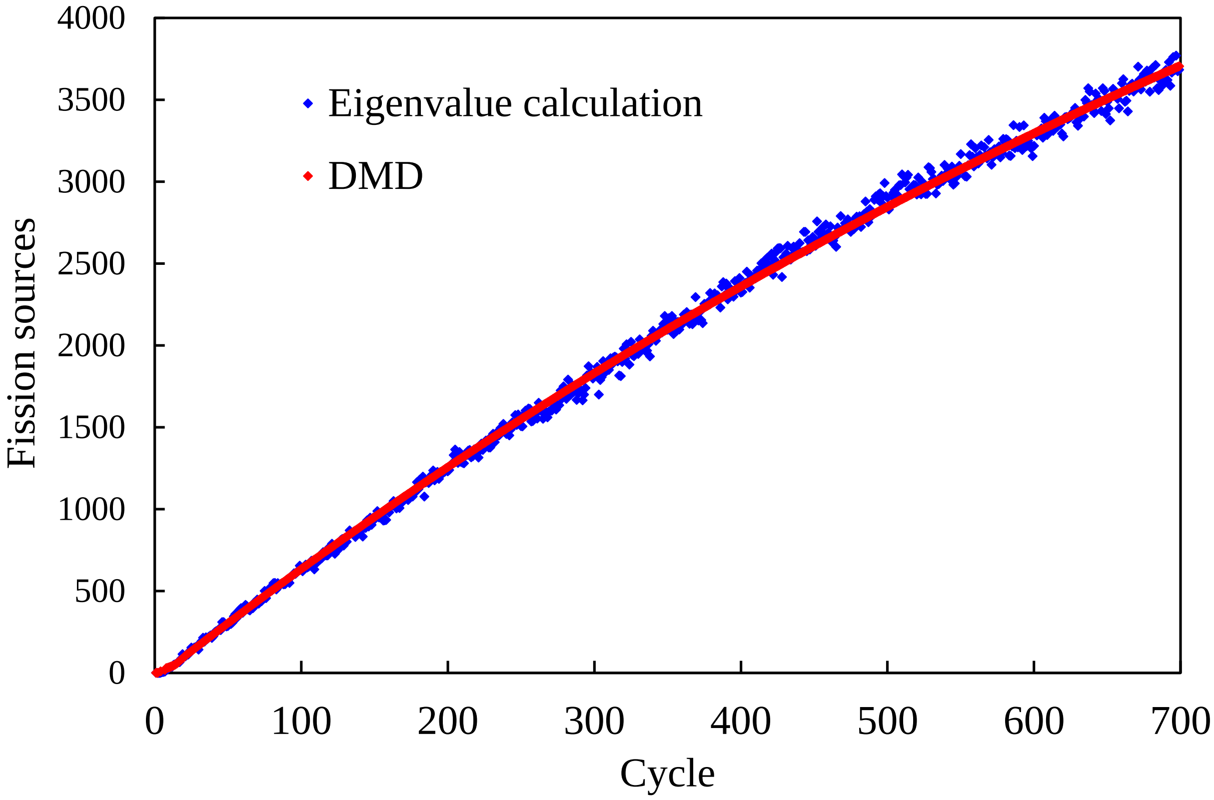

Fig. 16 Fission source transition that was reconstructed by the DMD method in Case 3 at the most remote position from the initial fission source

4.5 Results for Case 4 ($\rho \approx 0.996$) (Very large system of a single material)

This example had very large dimensions. In this large system, not only the dominance ratio (k_1/k_0) but also various other eigenvalue ratios ($k_i/k_0,\ i = 2, 3, \ldots$) were close to unity. The fission source convergence was dominated by the decay of several eigenmodes, including the 1st mode. The power iteration was performed in the same manner as in Case 3 up to the 700th cycle.

The fission source convergence at two positions is shown in Fig. 17 for 12 × 12 × 12 tally regions. The system dimensions were much larger than the neutron's mean free path. Thus, as shown in Fig. 17, very few neutrons reached the most remote position from the initial source position until the 200th cycle. Since several eigenmodes survived for many cycles in this large system, the elbow that was observed in Case 3 (see Fig. 11) was not observed in this large system.

Fig. 18 shows the dominance ratio ρ vs. rank r for several initial cycles I, where the last cycle was fixed at L = 700. According to Fig. 18, r = 30, I = 30, and L = 700 were identified as an optimal combination of the parameters. Figs. 19 and 20 show the dependence of the dominance ratio on the initial cycle *I* and last cycle *L*, respectively, for $r = 30$.

The dominance ratios that were obtained using the DMD method for several segmentations of tally regions (12 × 12 × 12, 6 × 6 × 6, 4 × 4 × 4, and 2 × 2 × 2) are listed in Table 4. Whereas the high dominance ratio system in Case 3 was insensitive to the parameters *r*, *I*, and *L*, the dominance ratio in Case 4 was more sensitive to these parameters. In particular, as shown in Fig. 20, the last cycle *L* should be larger in this type of large system, where the convergence is very slow. In contrast to Case 3, FMM did not produce satisfactory results even with 12 × 12 × 12 tally regions, thereby suggesting that further refinement of the tally regions was needed for the FMM.

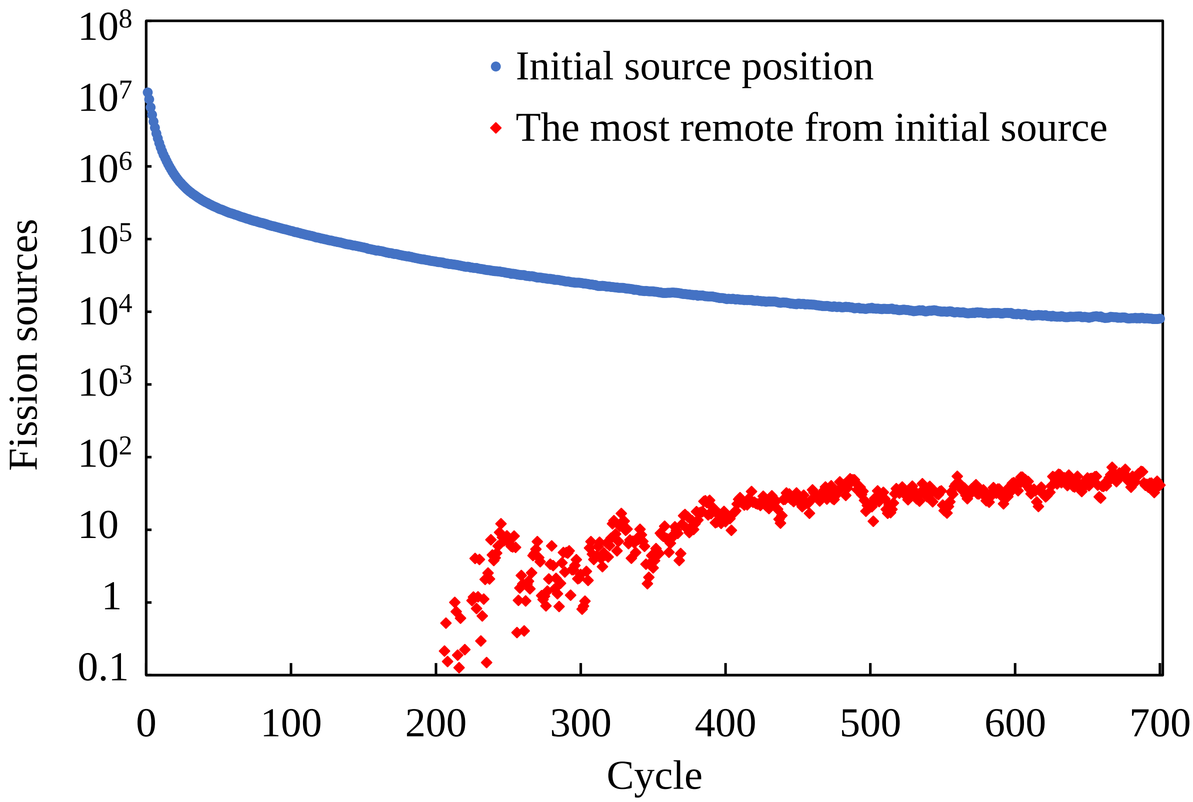

Fig. 17 Fission source convergence in Case 4

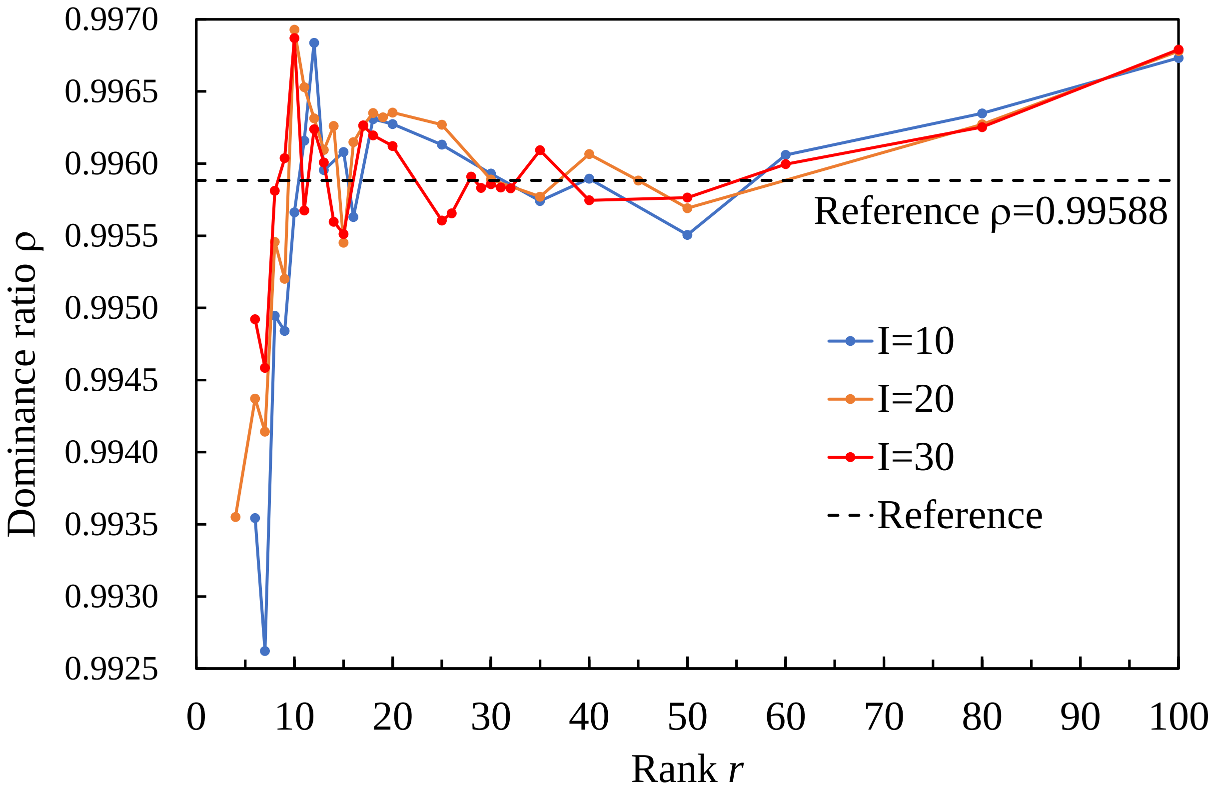

Fig. 18 Dominance ratio vs. rank *r* in Case 4

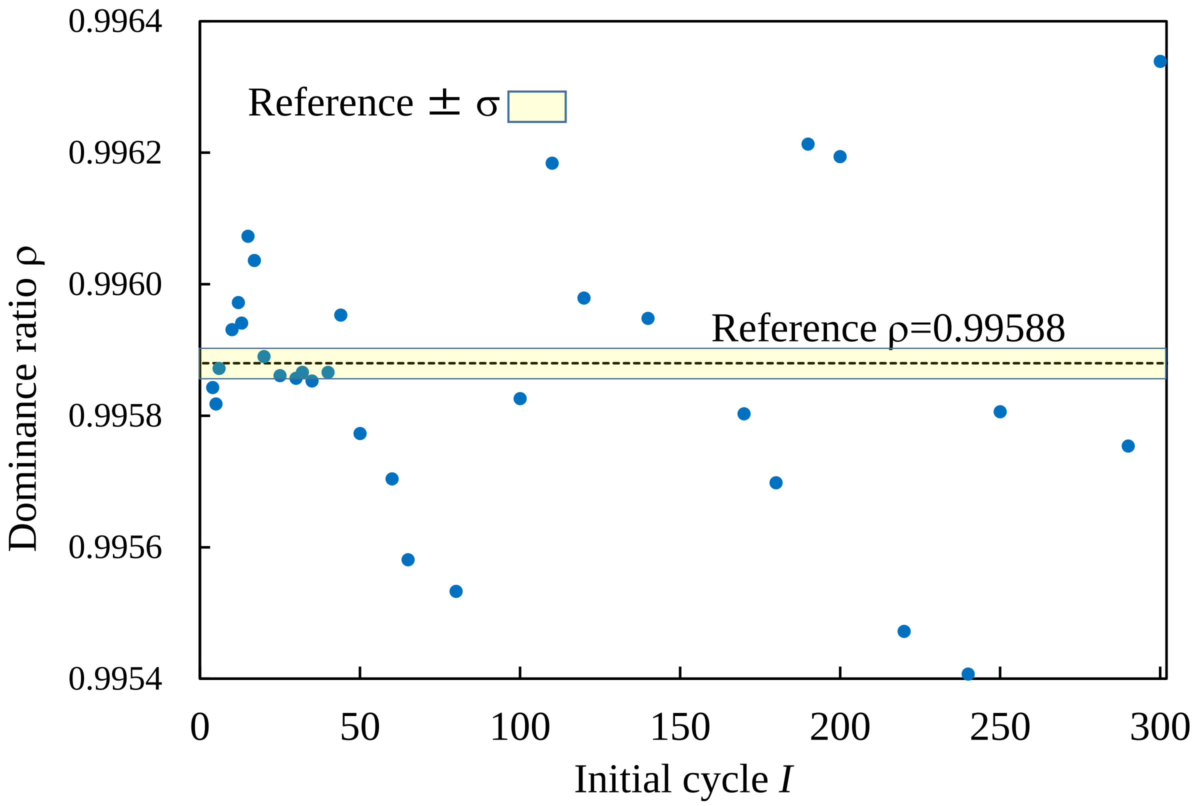

Fig. 19 Dominance ratio vs. initial cycle *I* in Case 4 (r = 30)

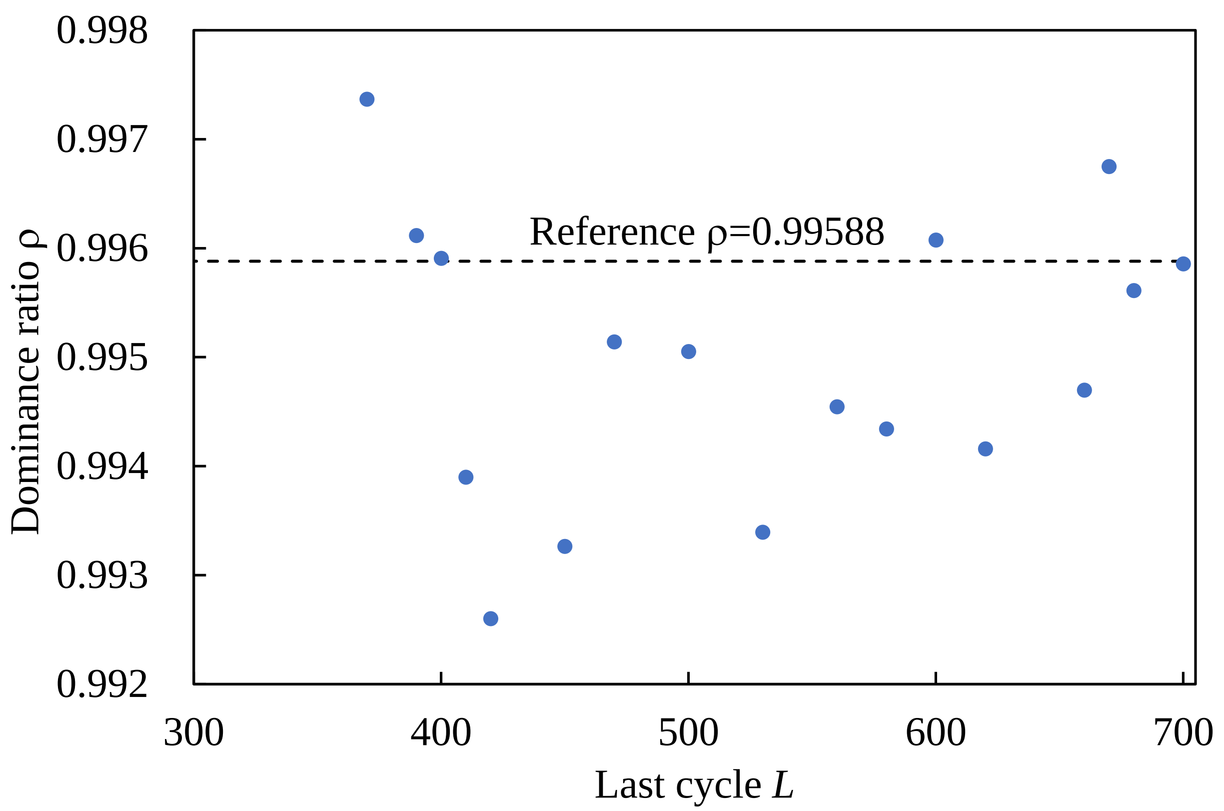

Fig. 20 Dominance ratio vs. last cycle L in Case 4 (r = 30)

4.6 Dominance ratio with a realistic number of neutrons per cycle

In the calculations in Sections 4.2~4.5, the number of fission source neutrons per cycle was set to be 12,000,000, which is much larger than that of ordinary criticality calculations, to reduce the random noise in the converging fission source. In this section, the dominance ratios were calculated with a much smaller number of source neutrons to investigate the effect of the random noise on accuracy of the DMD method. Here the number of initial source neutrons per cycle was set to be 200,000. The dominance ratio was estimated independently for 30 times for each case with difference random number seeds. The same parameters of rank r, initial cycle I, and last cycle L as those in Table 4 were used in the estimation calculations. The mean values and standard deviations of the 30 estimates of the dominance ratio are listed in Table 5. The comparison of the standard deviations of DMD-obtained dominance ratio between Tables 4 and 5 shows that, as the number of neutrons per cycle decreases, the fluctuation of the dominance ratio around the mean value increases significantly. As shown in Table 5, when the dominance ratio was nearly unity, the mean value was close to the reference value. However, in a low dominance system such as

Case 2 ($\rho \approx 0.721$), the mean value significantly deviated from the reference value and the standard deviation was especially great. As pointed out in (Yamamoto and Sakamoto, 2021), DMD method yields a biased result if the snapshot data used for a DMD analysis include the statistical fluctuation. For assessing an accurate unbiased dominance ratio, the number of source neutrons per cycle should be as large as possible. The Monte Carlo calculation for dominance ratio assessment need not be performed for many cycles after the fission source convergence. In some cases, the calculation can be terminated before convergence. Hence, dominance ratio assessment using a large number of source neutrons per cycle would not be so computationally expensive as *k*-eigenvalue calculations where many cycles need to be performed after the fission source convergence.

Table 5 Mean value and standard deviation of dominance ratios by DMD with 200,000 neutrons per cycle

Case	Tally region	r	I	L	Dominance ratio ρ DMD	Reference
1	12 × 12 × 12	15	4	100	0.90722 ± 0.00437	0.90673 ± 0.00005
	6 × 6 × 6	15	4	100	0.90773 ± 0.00407	
	4 × 4 × 4	15	4	100	0.90689 ± 0.00524	
	2 × 2 ×2	8	4	100	0.90917 ± 0.00430	
2	12 × 12 × 12	16	3	100	0.70227 ± 0.03000	0.72128 ± 0.00005
	6 × 6 × 6	16	3	100	0.70301 ± 0.03757	
	4 × 4 × 4	16	3	100	0.70819 ± 0.03398	
	2 × 2 ×2	8	3	100	0.69870 ± 0.03564	
3	12 × 12 × 12	30	35	700	0.99907 ± 0.00040	0.99915 ± 0.00004
	6 × 6 × 6	30	35	700	0.99909 ± 0.00042	
	4 × 4 × 4	30	35	700	0.99911 ± 0.00045	
	2 × 2 ×2	8	25	700	0.99917 ± 0.00044	
4	12 × 12 × 12	30	30	700	0.99505 ± 0.00180	0.99588 ± 0.00002
	6 × 6 × 6	30	30	700	0.99506 ± 0.00178	
	4 × 4 × 4	30	30	700	0.99535 ± 0.00189	
	2 × 2 ×2	8	30	700	0.99704 ± 0.00118	

4.7 How to select parameters *I*, *L*, and *r*

In this section, how to select the initial cycle I, last cycle L, and rank r is discussed and their recommendations are made. The initial cycle I should be larger than the cycle where the second and higher modes almost vanish. The last cycle L should be larger than the cycle where the fission source distribution reaches the convergence. The rank r should be determined by increasing r one by one from $r = 1$ until the dominance ratio becomes stable. These recommendations are preliminary ways and needs to be further investigated in the future.

For accurate assessment of dominance ratio, the initial cycle I, last cycle L, and rank r should be suitably determined. The determination of these parameters depends on the dominance ratio, which means that an approximate dominance ratio needs to be known beforehand. The dominance ratio can be approximately estimated by performing a criticality calculation and subsequent DMD analysis with roughly determined values of the parameters, I, L, and r. For example, $I = 1$, $r = \min(n, J-1)$, and $L =$ approximate cycles for source convergence can be candidates to obtain a roughly estimated dominance ratio.

5. Conclusions

The transition state of the fission source distribution toward convergence in a Monte Carlo k-eigenvalue calculation can be used for DMD analyses for dominance ratio assessment. The proposed method for dominance ratio assessment can be applied with a general-purpose Monte Carlo code if the code has a function to output fission sources for each cycle in discretized regions.

The dominance ratio that is obtained from the DMD method depends on the following parameters: the initial and last cycles that are used for the snapshots, the rank, and the spatial discretization of fission source tally regions. Using suitably chosen parameters (the initial and last cycles and the rank), the DMD method yields a reliable result for the dominance ratio. Compared to the FMM, the spatial discretization of the fission source tally regions for DMD analyses need not be fine. The dominance ratio that is obtained from the DMD method is insensitive to the number of tally regions, as with the CMPM and NPMM.

In a very high dominance ratio system in which two fissioning regions are separated from each other and many cycles are required for convergence, the dominance ratio that is obtained from the DMD method is insensitive to the initial and last cycles and the rank. Almost consistent results can be obtained from the DMD analyses regardless of these parameters. In contrast, in a low dominance ratio system in which the fission source converges rapidly in a very small number of cycles, the result for the dominance ratio depends significantly on these parameters. Hence, they should be suitably determined when DMD is used for dominance ratio assessment. The difficulty in a low dominance ratio system is caused by the reduced number of cycles before convergence that are used for DMD analyses. The development of decelerating fission source convergence, which increases the number of cycles before convergence, would effectively overcome this difficulty.

References

Abdo, M., Elzohery, R., Roberts, J.A., 2019. Modeling isotopic evolution with surrogates based on dynamic mode decomposition. Ann. Nucl. Energy 129, 280–288. https://doi.org/10.1016/j.anucene.2019.01.048.

Booth, T.E., 2003. Computing the higher *k*-eigenfunctions by Monte Carlo power iteration: a conjecture. Nucl. Sci. Eng. 143, 291–300. https://dx.doi.org/10.13182/NSE02-10TN.

Booth, T.E., 2006. Power iteration method for the several largest eigenvalues and eigenfunctions. Nucl. Sci. Eng. 154, 48–62. https://doi.org/10.13182/NSE05-05.

Carney, S., Brown, F. Kiedrowski, B., Martin, W., 2014. Theory and application of the fission matrix method for continuous-energy Monte Carlo. Ann. Nucl. Energy 73, 423–431. https://dx.doi.org/10.1016/j.anucene.2014.07.020.

Dawson, S.T.M., Hemati M.S., Williams, M.O., Rowley, C.W., 2016. Characterizing and correcting for the effect of sensor noise in the dynamic mode decomposition. Exp. Fluids 57:42. https://link.springer.com/article/10.1007/s00348-016-2127-7.

Di Ronco, A., Introini, C., Cervi, E., Lorenzi, S., Jeong, Y.S., Seo, S.B., Bang, I.C., Giacobbo, F., Cammi, A., 2020. Dynamic mode decomposition for the stability analysis of the molten salt fast reactor core. Nucl. Eng. Des. 362, 110529. https://doi.org/10.1016/j.nucengdes.2020.110529.

Dufek, J., Gudowski, W., 2009. Fission matrix based Monte Carlo criticality calculations. Ann. Nucl. Energy 36, 1270–1275. https://doi.org/10.1016/j.anucene.2009.05.003.

Dumonteil, E., Courau, T., 2010. Dominance ratio assessment and Monte Carlo criticality simulations: dealing with high dominance ratio systems. Nucl. Technol. 172, 120–131. https://doi.org/10.13182/NT10-A10899.

Gorodkov, S.S., 2011. Using core symmetry in Monte Carlo dominance ratio calculations. Nucl. Sci. Eng. 168, 242–247. https://doi.org/10.13182/NSE10-37.

Hardy, Z.K., Morel, J.E., Ahrens, C., 2019. Dynamic mode decomposition for subcritical metal systems. Nucl. Sci. Eng. 193 1173–1185. https://doi.org/10.1080/00295639.2019.1609317.

Kutz, J.N., Brunton, S.L., Proctor, J.L., 2016. Dynamic mode decomposition: Data-driven modeling for complex systems, Society for Industrial and Applied Mathematics, Philadelphia, Pennsylvania. https://doi.org/10.1137/1.9781611974508.

McClarren, R.G., 2019. Calculating time eigenvalues of the neutron transport equation with dynamic mode decomposition. Nucl. Sci. Eng. 193, 854–867. https://doi.org/10.1080/00295639.2018.1565014.

McClarren, R.G., Haut, T.S., 2020. Data-driven acceleration of thermal radiation transfer calculations with the dynamic mode decomposition and a sequential singular value decomposition. arXiv preprint arXiv:2009.11686.

Nease, B.R., Ueki, T., 2007. Time series analysis of Monte Carlo fission sources–III: coarse-mesh projection. Nucl. Sci. Eng. 157, 51–64. https://dx.doi.org/10.13182/NSE07-A2712.

Nease, B.R., Ueki, T., 2009. Time series analysis and Monte Carlo method for eigenvalue separation in neutron multiplication problems. J. Comput. Phys. 228, 8525–8547. https://dx.doi.org/10.1016/j.jcp.2009.07.037.

Okumura, K., Kugo, T., Kaneno K, Tsuchihashi, K., 2007. SRAC2006: A comprehensive neutronics calculation code system. JAEA-Data/Code 2007-004.

Penrose, R., 1955. A generalized inverse for matrices. Math. Proc. Camb. Philos. Soc. 51, 406–413. https://dx.doi.org/10.1017/S0305004100030401.

Roberts, J.A., Xu, L., Elzohery, R., Abdo, M., 2019. Acceleration of the power method with dynamic mode decomposition. Nucl. Sci. Eng. 193, 1371–1378. https://doi.org/10.1080/00295639.2019.1634928.

Schmid, P.J., 2010. Dynamic mode decomposition of numerical and experimental data. J. Fluid Mech. 656, 5–28. https://doi.org/10.1017/S0022112010001217.

Sutton, T.M., Romano, P.K., Nease, B.R., 2011. On-the-fly Monte Carlo dominance ratio calculation using the noise propagation matrix. Prog. Nucl. Sci. Technol. 2, 749–756. https://doi.10.15669/pnst.2.749.

Terlizzi, S., Kotlyar, D., 2019. Fission matrix decomposition method for criticality calculations: theory and proof of concept. Nucl. Sci. Eng. 193, 948–965. https://doi.org/10.1080/00295639.2019.1583948.

Ueki, T., Brown, F., Parsons, D.K., Kornreich, D.E., 2003. Autocorrelation and dominance ratio in Monte Carlo criticality calculations. Nucl. Sci. Eng. 145, 279–290. https://doi.org/10.13182/NSE03-04.

Ueki, T., Brown, F.B., Parsons, D.K., Warsa, J.S., 2004. Time series analysis of Monte Carlo fission sources–I: dominance ratio computation. Nucl. Sci. Eng. 148, 374–390. https://dx.doi.org/10.13182/NSE03-95.

Yamamoto, T., Miyoshi, Y., 2004. Reliable method for fission source convergence of Monte Carlo criticality calculations with Wielandt’s method. J. Nucl. Sci. Technol. 41, 99–107. https://dx.doi.org/10.1080/18811248.2004.9715465.

Yamamoto, T., 2009. Convergence of the second eigenfunction in Monte Carlo power iteration. Ann. Nucl. Energy 36, 7–14. https://dx.doi.org/10.1016/j.anucene.2008.11.004.

Yamamoto, T., Sakamoto, H., 2020. Convergence characteristics and Wielandt acceleration of the time source method for Monte Carlo alpha eigenvalue calculations. Ann. Nucl. Energy 146, 107627. https://doi.org/10.1016/j.anucene.2020.107627.

Yamamoto, T., Sakamoto, H., 2021. Application of dynamic mode decomposition to exponential experiment for spatial decay constant determination. Ann. Nucl. Energy 162, 108506.

https://dx.doi.org/10.1016/j.anucene.2021.108506.

Yamamoto, T., Sakamoto, H., 2022. Higher harmonic analyses of the Rossi-α method and application of dynamic mode decomposition for time decay constant determination in a 1D subcritical system. Ann. Nucl. Energy (in press). https://doi.org/10.1016/j.anucene.2021.108886.

Zhang, P., Lee, H., Lee, D., 2016. A general solution strategy of modified power method for higher mode solutions. J. Comput. Phys. 305, 387–402. https://dx.doi.org/10.1016/j.jcp.2015.10.042.

Zhang, P., Lee, H., Lee, D., 2018. On the transfer matrix of the modified power method. Comput. Phys. Commun. 222, 102–112. https://doi.org/10.1016/j.cpc.2017.09.022.

List of figures

fission source position

Fig. 16 Fission source transition that was reconstructed by the DMD method in Case 3 at the most remote position from the initial fission source

Fig. 17 Fission source convergence in Case 4

Fig. 18 Dominance ratio vs. rank *r* in Case 4

Fig. 19 Dominance ratio vs. initial cycle *I* in Case 4 (*r* = 30)

Fig. 20 Dominance ratio vs. last cycle *L* in Case 4 (*r* = 30)